On the Effect of Interference and Misalignment Error in Mixed RF/FSO Systems over Generalized Fading Channels

Abhijeet Upadhya, Vivek K. Dwivedi, *Member, IEEE,* and George K. Karagiannidis, *Fellow, IEEE*

***Abstract*—In this paper, the end-to-end performance of a mixed radio frequency (RF)/free space optical (FSO) affected by co-channel interference (CCI), is studied. We consider that the RF link experiences $\eta - \mu$ fading and the FSO link is subjected to atmospheric turbulence, which is modeled by the $\alpha - \mu$ distribution. Also, the statistics of the FSO link is presented for the case of zero and non-zero boresight pointing errors. Furthermore, we assume intensity modulation with direct detection (IM/DD) and coherent demodulation. In particular, we present a closed-form expression for the probability density function of the FSO link, which is then used to obtain a closed-form and an asymptotic expression for the outage probability. In order to quantify the system performance, we utilize this asymptotic result to yield the system's coding gain and diversity order. Moreover, we have presented analytical expressions for the average bit error rate (BER) and ergodic capacity for the system design. In order to gain more insights, high signal-to-noise ratio (SNR) approximations expressions for the BER and ergodic capacity, are also derived. Finally, the analytical results presented in the paper are validated through computer simulations.**

***Index Terms*—Free-space optical (FSO) communication, α-μ distribution, non-zero boresight pointing error, co-channel interference, Fox's H-functions.**

I. Introduction

In the last years, free space optical (FSO) communications is gaining high popularity as an efficient alternative technology to the scarcity of the available radio frequency (RF) spectrum. FSO systems keep the cost of installation low and can support more users with less power, due to the huge license-free bandwidth available in the optical spectrum [1]. Because of these favorable characteristics, FSO systems have been proposed for backbone and last-mile networks [1]. However, FSO faces a major challenge from the atmospheric turbulence (also known as *scintillation*) resulting from the change in the refractive index of the medium [2]. This phenomenon causes rapid fluctuations in the phase and intensity of the optical signal. In addition to the atmospheric turbulence, another impairment is the pointing error, which also degrades the system's quality-of-service (QoS). This is due to the building sway from dynamic wind loads and/or weak earthquakes, that leads to a misalignment between the transmitter beam and the receiver aperture [1].

Abhijeet Upadhya and Vivek K. Dwivedi are with department of Electronics and Communication Engineering, Jaypee Institute of Information Technology, Noida, India, (Email: upadhya.abhijeet@gmail.com, vivek.dwivedi@jiit.ac.in).

George K. Karagiannidis is with the Aristotle University of Thessaloniki, Thessaloniki, Greece (email: geokarag@auth.gr).

A. Literature

In order to overcome the detrimental effects mentioned above, relaying has been proposed for the FSO networks [3]–[8], where the signal from the source is relayed through several intermediate terminals to the destination node. Thus, it provides robustness to fading conditions, without increasing the physical size of the user terminals. Moreover, mixed RF/FSO relaying system, where both hops experience different channel conditions in terms of fading, has the capability to multiplex multiple RF users on the high bandwidth FSO channel, resulting in increased system capacity. In [3], the effect of turbulence on the outage performance of mixed RF/FSO amplify-and-forward (AF) relaying systems using subcarrier intensity modulation (SIM), was presented. It is worth mentioning that in AF relaying, the relay node simply amplifies the received signal and retransmits it towards the destination node, whereas the relay node in decode-and-forward (DF) relaying decodes, re-modulates and retransmits the information symbol to the destination. So, the processing overhead is significantly higher in case of DF relaying technique, which increases the overall cost of communication system. The authors in [4] have extended the work in [3] and analyze the performance in the presence of pointing errors in the FSO link. Furthermore, in [4], the RF hop was considered to undergo flat fading, modeled with Rayleigh distribution, while the high bandwidth FSO link was assumed to experience Gamma-Gamma atmospheric turbulence. In [5], the RF fading has been modeled with the Nakagami-m distribution, which is considered as more appropriate for wireless propagation environments, whereas the turbulence on the FSO link by the Gamma-Gamma distribution.

To further improve the mixed RF/FSO system performance, outdated channel state information (CSI) available at the relay node has been considered in [6] and analytical expressions are derived for the outage probability (OP). Additionally, the authors in [6] optimized the beam waist in order to minimize the effect of pointing error. The effect of eavesdropping on the mixed RF/FSO AF relaying has been presented in [7], where the authors have proposed a jamming model to accommodate secure transmission. Recently, the performance of fixed gain AF relaying in the presence of pointing error has been addressed in [8], by using the generalized $\mathcal{M}$-distribution to model the turbulence. This distribution include Gamma-Gamma and K-distribution as special cases.

Although the effect of turbulence and pointing error on the performance of FSO systems have been extensively

investigated in the open literature, an analysis on the effect of interference has been inadequately treated. However, the impact of interference is significant since FSO transmissions need to co-exist with different types of communication systems. Scanning the open literature, the impact of co-channel interference (CCI) on mixed RF/FSO relay networks was investigated in [9]–[13]. Specifically, the authors in [9] presented an outage and error rate analysis for mixed RF/FSO AF relaying systems, in the presence of CCI. An analysis of mixed RF/FSO systems with CCI, has been also presented in [10], where the RF user has been assumed to undergo Nakagami-m fading, whereas the irradiance fluctuation on the FSO link follows Gamma-Gamma distribution. Moreover, the authors of [11] have analyzed the ergodic capacity for a multi-aperture-FSO/multi-user-RF relay network. Additionally, the evaluation of mixed RF/FSO systems with relay selection, has been performed by Balti *et al* in [12], by including the effect of interference at the relay node. The same authors have analyzed the OP, bit error rate (BER) and ergodic capacity for the considered system. Recently, the authors of [13] have analyzed the performance of mixed RF/FSO relaying network in presence of co-channel interference at relay and destination nodes over α-μ atmospheric turbulence channels.

B. Motivation

Most of the research works [3]–[8] have assumed interference-free transmission for mixed RF/FSO relaying systems. However, it is important to note that mixed RF/FSO systems are vulnerable to interference, due to the involvement of the RF counterparts. Thus, the authors of [9]–[13] considered the effect of interference in mixed RF/FSO systems and model the RF link using Rayleigh or Nakagami-m model. However, these distributions lack the adaptability to deal with diverse signal propagation mechanisms and the effect of small-scale fading and shadowing has to be considered in order to accurately describe the system performance. This requires to model the RF channels with more generalized distributions as the $\eta-\mu$ fading model, proposed in [14], which includes Rayleigh, Nakagami-m, and Hoyt as special cases.

The effect of irradiance fluctuation on the FSO link has been addressed in most of aforementioned works, which assumed Gamma-Gamma fading. In general, most of the fading models presented in the open literature are based on the assumption of homogeneous diffused scattering, and thus, the non-linearity of the wireless channel is not considered [15]. In this model, the α parameter represents the non-linearity of the wireless medium, while the μ parameter refers to the number of multipath clusters [15]. Moreover, the validity of model has been verified against experimental data in [16]. As shown in [15], for different combinations of the model parameters, the $\alpha-\mu$ includes various distributions. It is important to note that the $\alpha-\mu$ model has been adopted to model turbulence on the FSO link in research works [13], [17]–[19] due to its generic nature.

In general, the pointing error consists of two components: boresight and jitter. The boresight component is the fixed displacement between beam center and center of the detector [20]. Previous research works in [3]–[13], [17]–[19] have analyzed the system performance by neglecting the non-zero boresight component of pointing error. Notably, in terrestrial FSO systems, the transceivers are generally placed at the top of high rise buildings to obtain line-of-sight. Due to thermal expansion of such high rise building, the boresight error is considerable and can not be neglected [20].

The works [9]–[13] have considered interference, but the analysis is different from that presented in this paper. Specifically, the authors of [9] have assumed the presence of a direct link between source and destination nodes and applied selection combining to evaluate the instantaneous signal-to-interference plus noise (SINR). Ehsan et al. in [9] have derived the expressions of OP and BER for the dual-hop AF relaying system, but have not included the results for capacity offered by the overall system. Further to this, the authors have neglected the boresight component of pointing errors in the analysis. Additionally, the authors of [10] have presented a closed form expression for the OP of the dual hop AF semi-blind relay networks in the presence of interference, neglecting the non-zero boresight errors. The analysis in [10] is focused on the OP analysis and no results were given for the error rate, capacity, coding gain and diversity order. Moreover, the authors of [11] analyze the ergodic capacity of the interference limited FSO/RF AF relaying system in the absence of boresight component of pointing errors. However, outage and error rate analysis were not presented in [11]. The authors of [12] have derived the expressions for the OP, BER and ergodic capacity of the mixed RF/FSO AF relaying systems. Neglecting the boresight pointing errors, the analysis in [12] has been performed by resorting to upper bound of the end-to-end SINR. Recently, in [13], the authors have studied the performance of user diversity aided mixed RF/FSO DF relaying. The analysis in [13] is restricted to OP and BER expressions only, and no results for coding gain, diversity order and capacity of the overall system have been presented.

It is important to note that the results presented in [9]–[13] have been performed by neglecting the boresight component of pointing errors. In addition to this, the results are obtained by assuming fading distributions on the RF and FSO links which are not generalized. To the best of authors' knowledge, no work has considered the effect of non-zero boresight pointing errors in the existing literature for interference-limited mixed RF/FSO AF relaying systems. Motivated from the above, in this work, we consider a mixed RF/FSO AF relaying system in the presence of interference, at the relay node, where the amplitude fluctuations of the RF channel is modeled with the $\eta-\mu$ distribution, and the atmospheric turbulence is assumed to follow $\alpha-\mu$ distribution. The model on the FSO link also considers the case of non-zero boresight pointing errors. Considering the presence of N-CCIs at the relay node, we present exact and asymptotic closed-form expressions for the OP, BER, ergodic capacity, coding gain and diversity order for both intensity modulation-direct detection (IM/DD) as well as for coherent demodulation schemes.

C. Contribution

More specifically, the key contributions of this paper can be summarized as follow:

- We propose a unified framework to analyze the performance of an interference limited mixed RF/FSO relaying network over generalized fading channels.
- First, we have derived the exact closed-form expressions for the PDF of instantaneous SNR on the FSO link with turbulence modeled as $\alpha-\mu$ distribution with pointing errors. The expression for the PDF have been presented for zero and non-zero boresight pointing errors. In addition to this, an approximate PDF on the FSO link over $\alpha-\mu$ turbulence model with non-zero boresight pointing errors, has been presented.
- The obtained statistics have been utilized to obtain exact closed-form expression for the OP of the interference-limited dual hop AF relaying system with non-zero boresight pointing errors on the FSO link.
- We further investigate the effect of non-zero boresight pointing errors on outage performance of the considered system by deriving an approximate expression for the OP. To this end, we formulate the asymptotic behavior of OP for non-zero boresight pointing errors.
- For the case of zero boresight errors, we derive a closed-form expression for the end-to-end OP by considering N CCIs at the relay node of the dual hop mixed RF/FSO AF relaying system. Then, we investigate the high SNR performance of the OP by deriving closed-form expressions for the system's coding gain and diversity order.
- New analytical as well as simple asymptotic expressions of end-to-end BER for a variety of binary modulation schemes are derived for zero boresight pointing error case. Additionally, we have presented an approximate BER expression for the considered system in the presence of non-zero boresight pointing errors.
- Moreover, we present a closed-form expression for the ergodic capacity of the mixed RF/FSO systems in the presence of interference, along with a simple asymptotic approximation.
- The generalization capability of the $\alpha-\mu$ model to model the strength of turbulence for different parameters, is also presented. Specifically, we have illustrated the OP and BER performance using $\alpha-\mu$ model as special case for log-normal, Gamma-Gamma and K-distribution, based on the generic nature of the $\alpha-\mu$ model.

D. Structure

The remainder of the paper is organized as follows. A closed-form expression for the PDF of wireless optical channel with pointing errors is derived in Section II. Exact and asymptotic closed form expressions for the OP, coding gain, diversity order, BER and ergodic capacity are presented in section III. The theoretical expressions of the section III are numerically evaluated and validated in section IV. Finally, section V presents some concluding remarks.

II. Channel and System Model

The considered asymmetric mixed RF/FSO AF cooperative relaying system is shown in Fig. 1. In the proposed system, source node (S) communicates with destination node (D) through the relay node (R), which is corrupted by N CCIs. At the relay node the RF signal is converted into the optical domain, which is transmitted on the FSO link towards the node D on the relay to destination (R-D) link. Both the hops of the fixed gain relaying scheme are considered to be affected by additive white Gaussian noise (AWGN).

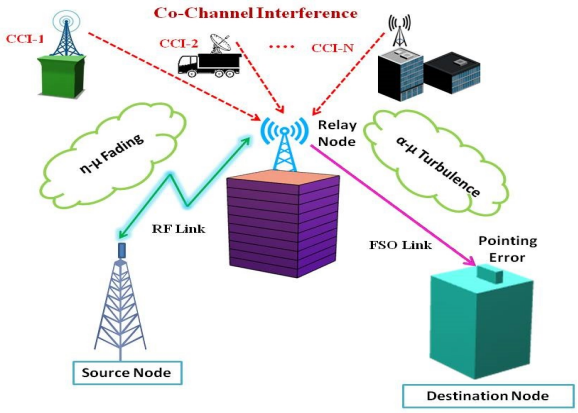

Fig. 1. A dual-hop amplify-and-forward RF/FSO relaying system in the presence of co-channel interference

A. RF Link Statistics

Next, the instantaneous signal-to-noise (SNR) on the S-R link is assumed to undergo $\eta-\mu$ fading [3]. The received signal at the relay node can be expressed as:

$$r_{sr} = h_{sr}x + \sum_{i=1}^{N} h_i x_i + N_{01} \tag{1}$$

where x is the RF information signal, h_{sr} is the $\eta-\mu$ distributed fading coefficient on the S-R link with power P_s, h_i is the fading amplitude of the i^{th} CCI channel and N_{01} represents AWGN with zero mean and variances σ_{sr}^2. The PDF of the instantaneous SNR is given by [14]

$$f_{\gamma_1}(\gamma_1) = \frac{2\sqrt{\pi}\mu_1^{\mu_1+\frac{1}{2}} h^{\mu_1}\gamma_1^{\mu_1-\frac{1}{2}}}{\Gamma(\mu_1)H^{\mu_1-\frac{1}{2}}\bar{\gamma}_1^{\mu_1+\frac{1}{2}}} I_{\mu_1,0.5}\left[\frac{2\mu_1 H\gamma_1}{\bar{\gamma}_1}\right] \tag{2}$$

where $\bar{\gamma}_1$ is the average SNR in the S-R link, $I_n[m]$ is the modified Bessel function of the first kind [21, Eq. (8.431.1)]. The parameters h and H can be defined based on the two formats proposed in [14], wherein, according to the first format $h = \frac{2+\eta^{-1}+\eta}{4}$ and $H = \frac{\eta^{-1}-\eta}{4}$, with $0 < \eta < \infty$. On the other hand, as per the second format, $h = \frac{1}{1-\eta^2}$ and $H = \frac{\eta}{1-\eta^2}$, with $-1 < \eta < 1$. For integer values of μ_1, the PDF of the SNR can be written as [22]

$$f_{\gamma_1}(\gamma_1) = \sum_{l=0}^{\mu_1-1} \mathcal{A}_1 \gamma_1^{\mu_1-l-1}[(-1)^l \exp(-a_1\gamma_1) + (-1)^{\mu_1}\exp(-a_2\gamma_1)] \tag{3}$$

where $\mathcal{A}_1 = \frac{\Gamma(\mu_1+l)\mu_1^{\mu_1-l}h^{\mu_1}}{\Gamma(\mu_1)l!\Gamma(\mu_1-l)4^l\bar{\gamma}_1^{\mu_1-l}H^{\mu_1+l}}$, $a_1 = \frac{2\mu_1(h-H)}{\bar{\gamma}_1}$ and $a_2 = \frac{2\mu_1(h+H)}{\bar{\gamma}_1}$. Moreover, the CDF of the instantaneous SNR on the RF link can be derived as

$$F_{\gamma_1}(\gamma_1) = \int_0^{\gamma_1} f_{\gamma_1}(y)dy \tag{4}$$

With the help of (3) and [21, Eq. (3.381.1)] holds that

$$F_{\gamma_1}(\gamma_1) = \sum_{l=0}^{\mu_1-1} \mathcal{A}_1 \Bigg[\mathcal{A}_2 \Big[1 - e^{-a_1\gamma_1} \sum_{m=0}^{\mu_1-l-1} \frac{(a_1\gamma_1)^m}{m!} \Big] + \mathcal{A}_3 \Big[1 - e^{-a_2\gamma_1} \sum_{m=0}^{\mu_1-l-1} \frac{(a_2\gamma_1)^m}{m!} \Big] \Bigg] \quad (5)$$

where $\mathcal{A}_2 = (-1)^l (a_1)^{-(\mu_1-l)} (\mu_1 - l - 1)!$ and $\mathcal{A}_3 = (-1)^{\mu}_{l} (a_2)^{-(\mu_1-l)} (\mu_1 - l - 1)!$.

Furthermore, we consider that the RF hop is affected by the presence of N Rayleigh distributed CCIs with total interference-to-noise ratio (INR) given by $\gamma_I = \sum_{i=1}^{N} \frac{{h_i}^2 P_I}{\sigma_{sr}^2}$, where P_I is the average power. The PDF of the sum of N-Rayleigh distributed random variables, which follow Chi-square distribution with $2N$ degree of freedom is given by [23]

$$f_{\gamma_I}(\gamma_I) = \frac{{\gamma_I}^{N-1}}{\bar{\gamma}_I^N (N-1)!} \exp\Big[- \frac{\gamma_I}{\bar{\gamma}_I} \Big] \quad (6)$$

In (6), the average INR per CCI link is, $\bar{\gamma}_I = \mathbb{E}\left[\frac{{h_i}^2 P_I}{\sigma_{sr}^2} \right]$.

B. FSO Link Statistics

The overall channel state on the FSO link is consisted from three independent factors as $I = I_a I_p I_l$. The factor I_l is the deterministic path loss, I_a is the turbulence induced fading and I_p represents the pointing error caused by the misalignment between the transmitter and receiver apertures. The atmospheric loss is defined by the Beers Lambert Law as [24]

$$I_l(z) = \exp(-\sigma z) \quad (7)$$

where $I_l(z)$ is the path loss over a propagation length of z while σ is the attenuation coefficient. Generally, I_l is considered as a fixed scaling factor over a long period of time, with no fluctuations. The turbulence induced irradiance, I_a, of the FSO link can be modeled with the $\alpha - \mu$ distribution [17]–[19]

$$f_{I_a}(I_a) = \frac{\alpha \mu_2 {I_a}^{\alpha\mu_2 - 1}}{\Gamma(\mu_2) \hat{\omega}_a{}^{\alpha\mu_2}} \exp\left[- \mu_2 \left(\frac{I_a}{\hat{\omega}_a} \right)^{\alpha} \right] \quad (8)$$

where $\hat{\omega}_a = \sqrt[\alpha]{\mathbb{E}(I_a^{\alpha})}$ is the α-root mean value of atmospheric turbulence random variable, while α and μ_2 are model parameters.

1) Pointing Error With Zero Boresight: The reliability and link performance of the line-of-sight FSO system depends upon the alignment between the optical transmitter and the receiver aperture. In [1], the authors have presented a pointing error model for a Gaussian beam profile. The pointing error parameter ξ is defined as $\xi = \frac{w_{z_{eq}}}{2\sigma_s}$ [1], where $w_{z_{eq}}$ is the equivalent beam waist at a distance of z defined by the relation $w_{z_{eq}}^2 = \frac{w_z^2 \sqrt{\pi} erf(v)}{2v \exp(-v^2)}$, $v = \frac{\sqrt{\pi} r}{2 b_z}$ where w_z is the beam waist (calculated at e^{-2}) of the Gaussian spatial beam profile. The fraction of the power collected at a distance of $z = 0$ is given by $A_0 = [\mathrm{erf(v)}]^2$. The pointing error parameter $\xi \to \infty$ for the case of no misalignment error and smaller values of the parameter corresponds to a greater value of pointing error. Considering path loss, scintillation and pointing error the combined channel statistics on the FSO link may be obtained using

$$f(I) = \int f_{I/I_a}\Big(I/I_a \Big) f(I_a) dI_a \quad (9)$$

where the conditional PDF is defined as

$$f_{I/I_a}\Big(I/I_a \Big) = \frac{1}{I_a I_l} f_{I_p}\Big(\frac{I}{I_a I_l} \Big) \quad (10)$$

By using [21, Eq. (3.383.1)], the integral in (10) can be solved as [19]

$$f(I) = \frac{\xi^2}{\Gamma(\mu_2)} \left(\frac{\mu_2}{A_o \hat{\omega}_a I_l} \right)^{\frac{d}{2}} W_{\frac{\alpha\mu_2 - \xi^2 - \alpha}{2\alpha}, \frac{\xi^2 - \alpha\mu_2}{2\alpha}} \left(\frac{\mu_2}{\hat{\omega}_a^{\alpha}} \right) I^{\frac{d}{2}-1} \times \exp\Big[- \frac{\mu_2}{2} \left(\frac{I}{A_o \hat{\omega}_a} \right)^{\alpha} \Big] \quad (11)$$

where $d = \xi^2 + \alpha\mu_2 - \alpha$ and $W_{a,b}(c)$ is the Whittaker function defined in [21, Eq. (9.220.4)]. The v^{th} moment of the normalized envelope of irradiance random variable I_a is given by [15]

$$\mathbb{E}^v[\mathrm{I}_a] = \frac{\Gamma(\mu_2 + \frac{v}{\alpha})}{(\mu_2)^{\frac{v}{\alpha}} \Gamma(\mu_2)} \quad (12)$$

where $\mathbb{E}[.]$ denotes expectation. Using (12), the scintillation index (SI) can be readily calculated as

$$\sigma_I^2 = \frac{\mathbb{E}[\mathrm{I}^2]}{\mathbb{E}^2[\mathrm{I}]} - 1 \underset{\xi^2 \gg 1}{=} \frac{\Gamma(\mu_2)\Gamma(\mu_2 + \frac{2}{\alpha})}{(\mu_2)^{\frac{1}{\alpha}} \left[\Gamma(\mu_2 + \frac{1}{\alpha}) \right]^2} \left(\frac{\xi^2}{\xi^2 + 2} \right) - 1 \quad (13)$$

The value of SI σ_I^2 defined in (13) can be compared with [25, Eq. (7), Eq. (9)] to obtain Rytov variance σ_1^2 which can be directly related to the strength of atmospheric turbulence. The Rytov variance is defined by $\sigma_1^2 = 1.23 C_n^2 k^{\frac{7}{6}} L^{\frac{11}{6}}$, where C_n^2 denotes the refraction structure parameter, $k = \frac{2\pi}{\lambda}$ is the optical wave number, λ is the signal wavelength and L is the link distance. Importantly, the generalization property of the $\alpha - \mu$ distribution can be utilized with the help of [15] as

$$\frac{\Gamma^2\left(\mu_2 + \frac{1}{\alpha}\right)}{\Gamma(\mu_2)\Gamma\left(\mu_2 + \frac{2}{\alpha}\right) - \Gamma^2\left(\mu_2 + \frac{1}{\alpha}\right)} = \frac{\mathbb{E}^2[I_a]}{\mathbb{E}[{I_a}^2] - \mathbb{E}^2[I_a]} \quad (14)$$

and

$$\frac{\Gamma^2\left(\mu_2 + \frac{2}{\alpha}\right)}{\Gamma(\mu_2)\Gamma\left(\mu_2 + \frac{4}{\alpha}\right) - \Gamma^2\left(\mu_2 + \frac{2}{\alpha}\right)} = \frac{\mathbb{E}^2[{I_a}^2]}{\mathbb{E}[{I_a}^4] - \mathbb{E}^2[{I_a}^2]} \quad (15)$$

The system of transcendental equations in (14) and (15) have been presented in [15] as moment-based estimators for the parameters α and μ of the distribution. Therefore, for a given irradiance PDF, the value of model parameters can be obtained by evaluating first, second and forth moments of any given statistics such as Gamma-Gamma [3]–[5], K-distribution [26] and log-normal distribution [27]. Moreover, the system of equations can be solved using mathematical softwares such as MATLAB and Mathematica.

The irradiance statistics in (11) can be represented in terms of electrical SNR Ψ_2 using transformation $\bar{\Psi}_2 = \frac{(\eta \mathbb{E}[I])^2}{N_{02}}$ where $\bar{\Psi}_2$ is the average electrical SNR on the FSO link for IM/DD

receiver. Using the relation $\gamma = \frac{(\eta I)^2}{N_{02}}$, with $\frac{\eta^2}{N_{02}} = \frac{\bar{\Psi}_2}{\mathbb{E}[I]^2}$ for IM/DD detection, and the average SNR on the FSO link $\bar{\Psi}_1$ is defined as $\bar{\Psi}_1 = \frac{\eta \mathbb{E}[I]}{N_{02}}$ for coherent detection. Applying the transformation, the unified PDF of electrical SNR on the FSO link can be obtained as [19]

$$f(\gamma) = \mathcal{A}_4 \gamma^{\frac{d}{2\rho}-1} \exp\left[-\mathrm{B}\gamma^{\frac{\alpha}{\rho}}\right] \tag{16}$$

where $\mathrm{B} = \frac{\mu_2}{2}(\Omega_2 \hat{\omega}_a A_o)^{-\alpha}$, $\rho = 1$ corresponds to coherent demodulation technique while $\rho = 2$ represents the IM/DD detection of optical signal with $\Omega_\rho = \frac{(\bar{\Psi}_\rho)^{\frac{1}{\rho}}}{\mathbb{E}[\mathrm{I}]}$. Further, the constant $\mathcal{A}_4$ is defined by the relation $\mathcal{A}_4 = \frac{\xi^2}{\rho\Gamma(\mu_2)}\left(\frac{\mu_2}{\Omega_\rho A_o \hat{l}_a}\right)^{\frac{d}{2}} W_{\frac{\alpha\mu_2-\xi^2-\alpha}{2\alpha}, \frac{\xi^2-\alpha\mu_2}{2\alpha}}\left(\frac{\mu_2}{\hat{l}_a^{\alpha}}\right)$.

2) Pointing Error With Non-Zero Boresight: In order to add practicality to the proposed system model, the analysis on the FSO link is extended to consider the case of non-zero boresight pointing error. The PDF of I_p with non-zero boresight pointing errors is given as [20]

$$f_{I_p}(I_p) = \frac{\xi^2}{A_o^{\xi^2}} \exp\left(-\frac{\tau^2}{\sigma_s^2}\right) I_p^{\xi^2-1} I_0\left(\frac{\tau}{\sigma_s}\sqrt{-2\xi^2 \ln\left(\frac{I_p}{A_o}\right)}\right), \quad 0 < I_p < A_o \tag{17}$$

where τ denotes the boresight displacement and $I_0(.)$ is the modified Bessel function of the first kind and zero order defined in [21, 8.431.1]. It is important to note that for $\tau = 0$, the pointing error model in (17) specializes for the case of zero-boresight error. Moreover, the v^{th} moment of I_p for non-zero boresight can be expressed as [20]

$$\mathbb{E}^v[\mathrm{I}_p] = \frac{A_o^v \xi^2}{v+\xi^2} \exp\left(-\frac{v\tau^2}{2\sigma_s^2(v+\xi^2)}\right) \tag{18}$$

For combining the effect of atmospheric turbulence with non-zero pointing error, the statistics on the FSO link can be obtained using the relationship $f(I) = \int f_{I/I_a}\left(I/I_a\right) f(I_a) dI_a$. Substituting (17) and (8), the overall irradiance can be further written as

$$f(I) = \frac{\xi^2 \alpha \mu_2}{\Gamma(\mu_2)\hat{\omega}_a A_o^{\xi^2}} \exp\left(-\frac{\tau^2}{2\sigma_s^2}\right) I^{\xi^2-1} \int_{I/A_o}^{\infty} I_a^{\alpha\mu_2-\xi^2-1} \times \exp\left(-\frac{\mu_2}{\hat{\omega}_a{}^{\alpha} I_a^{\alpha}}\right) I_0\left(\frac{\tau}{\sigma_s}\sqrt{-2\xi^2 \ln\left(\frac{I}{I_a A_o}\right)}\right) dI_a \tag{19}$$

Using the method given in Appendix A, a closed-form expression for PDF of irradiance fluctuation on FSO link with non-zero boresight error can be derived as

$$f(I) = \frac{\xi^2}{\Gamma(\mu_2)} \exp\left(-\frac{\tau^2}{2\sigma_s^2}\right) \sum_{m_1=0}^{n} \hat{b}_{m_1,n,0} \left(\frac{\xi}{\sqrt{2\alpha\sigma_s}}\tau\right)^{2m_1} \times (-1)^{m_1} \frac{\partial^{m_1}}{\partial s^{m_1}} \left\{\frac{\mu_2^{s+1}}{(A_o\hat{\omega})^{\alpha\mu_2+\alpha s}} I^{\alpha\mu_2+\alpha s} \Gamma\left(-s, \frac{\mu_2}{(\hat{\omega}A_o)^{\alpha}} I^{\alpha}\right)\right\} \tag{20}$$

where $s = (\xi^2 - \alpha\mu)/\alpha$ and

$$\hat{b}_{m_1,n,v} = (-1)^{m_1} \frac{(n+m_1-1)!}{m_1!(n-m_1)!} \frac{n^{1-2m_1}}{\Gamma(v+m_1+1)} \tag{21}$$

After random variable substitution, the unified PDF of the atmospheric turbulence with nn-zero boresight pointing errors can be established as

$$f(\gamma) = \sum_{m_1=0}^{n} \Phi_1(m_1) \frac{\partial^{m_1}}{\partial s^{m_1}} \left\{\Phi_2(s) \gamma^{\frac{\alpha\mu_2+\alpha s}{\rho}-1} \Gamma\left(-s, \Phi_3 \gamma^{\frac{\alpha}{\rho}}\right)\right\} \tag{22}$$

where $\Phi_1(m_1) = (-1)^{m_1} \frac{\xi^2}{\rho\mu_2} \exp\left(-\frac{\tau^2}{2\sigma_s^2}\right) \hat{b}_{m_1,n,0} \left(\frac{\xi}{\sqrt{2\alpha\sigma_s}}\tau\right)^{2m_1}$ $\Phi_2(s) = \frac{\mu_2^{s+1}}{(A_o\hat{\omega}\Omega_\rho)^{\alpha\mu_2+\alpha s}}$ and $\Phi_3 = \frac{\mu_2}{(\hat{\omega}A_o\Omega_\rho)^{\alpha}}$.

An Approximation

In order to simplify the results, we approximate the PDF of the irradiance, in the presence of non-zero boresight error. After some mathematical manipulations, the expression of $f(I)$ in (19) can be further expressed as

$$f(I) = \frac{\alpha\mu_2}{\Gamma(\mu_2)(\hat{\omega}_a A_o)^{\alpha\mu_2}} \exp\left(-\frac{\tau^2}{2\sigma_s^2}\right) I^{\alpha\mu_2-1} \times \int_0^{\infty} z \exp\left(-\left(\frac{\xi^2-\alpha\mu_2}{2\xi^2}\right) z^2\right) \exp\left[-\mu_2\left(\frac{I}{\hat{\omega}A_o}\right)^{\alpha} \exp\left[\frac{\alpha}{2\xi^2} z^2\right]\right] \times I_0\left(\frac{\tau}{\sigma_s} z\right) dz \tag{23}$$

The exponential function in (19) can be represented in terms of Meijer-G using [28, Eq. (07.34.06.0014.01)] which can be substituted in (23) resulting in

$$f(I) = \frac{\alpha}{\Gamma(\mu_2)} \exp\left(-\frac{\tau^2}{2\sigma_s^2}\right) \sum_{m_2=0}^{J} \left[\mu_2^{m_2+1} \frac{I^{\alpha\mu_2+\alpha m_2-1}}{(\hat{\omega}_a A_o)^{\alpha\mu_2+\alpha m_2}}\right] \frac{\Gamma(m_2)}{(1)_{m_2}} \times \int_0^{\infty} z \exp\left(-\left\{\frac{\xi^2-\alpha\mu_2-\alpha m_2}{2\xi^2}\right\}\right) I_0\left(\frac{\tau}{\sigma_s} z\right) dz \tag{24}$$

where $(.)_i$ is the Pochhamer number such that $(a)_i = a(a+1)\ldots(a+i-1)$. The upper limit of the summation J is defined as $J = \left\lfloor \frac{\xi^2-\alpha\mu_2-\alpha m_2}{2\xi^2} \right\rfloor$, where $\lfloor x \rfloor$ denotes the greatest integer function. Moreover, on applying [21, Eq. (6.643.2)], the closed-form expression can be obtained as

$$f(I) = \frac{\alpha\mu_2\sigma_s}{\tau\Gamma(\mu_2)} \exp\left(\frac{-\tau^2}{2\sigma_s^2}\right) \sum_{m_2=0}^{J} \frac{\Gamma(m_2)\mu_2{}^{m_2}}{(\omega_a A_o)^{\alpha\mu_2+\alpha m_2}(1)_{m_2}} \times \exp\left(\frac{\tau^2}{8\sigma_s^2\Phi_4}\right) \Phi_4{}^{-0.5} M_{-\frac{1}{2},0}\left(\frac{\tau^2}{4\sigma_s^2\Phi_4}\right) I^{\alpha\mu_2+\alpha m_2-1} \tag{25}$$

where $\Phi_4 = \frac{\xi^2-\alpha\mu_2-\alpha m_2}{2\xi^2}$ and $M_{a,b}(c)$ represents Whittaker function defined in [21, 9.221]. After performing random variable transformation, the approximate statistics of SNR on the FSO link with non-zero boresight error can be expressed as

$$f(\gamma) = \Phi_5 \sum_{m_2=0}^{J} \Phi_6(m_2) \gamma^{\frac{\alpha\mu_2+\alpha m_2}{\rho}-1} \tag{26}$$

where $\Phi_5 = \frac{\alpha\mu_2\sigma_s}{\tau\rho\Gamma(\mu_2)} \exp\left(\frac{-\tau^2}{2\sigma_s^2}\right)$ and

$$\Phi_6(m_2) = \frac{\Gamma(m_2)\mu_2{}^{m_2}}{(\omega_a A_o \Omega_\rho)^{\alpha\mu_2+\alpha m_2}(1)_{m_2}} \exp\left(\frac{\tau^2}{8\sigma_s^2\Phi_4}\right) \Phi_4{}^{-0.5} \times M_{-\frac{1}{2},0}\left(\frac{\tau^2}{4\sigma_s^2\Phi_4}\right) \tag{27}$$

The simplicity of the approximate PDF will be later utilized to derived performance metrics of the system under study.

C. End-to-end SNR Statistics

Assuming N CCIs, $\{x_i\}_{i=1}^{N}$ at the relay node, each with RF power P_i, the received signal at the destination node is given by [10]

$$x_d = (I\eta')^{\frac{\rho}{2}} G\left(h_{sr}x + \sum_{i=1}^{N} h_i x_i + N_{01}\right) + N_{02} \tag{28}$$

where N_{02} represent AWGN on the R-D link with zero mean and variance σ_{rd}^2. The optical-to-electrical conversion ratio at the destination node is given by η' while the overall optical signal irradiance is denoted by I and the G denotes fixed gain of the relay node. Assuming the presence of instantaneous channel state information (CSI) at relay node R, the fixed gain G provided by the AF scheme can be selected as [10]

$$G^2 = \frac{P_t}{\mathbb{E}[h_{sr}^2]P_s + \sum_{i=1}^{N}\mathbb{E}[h_i^2]P_i + \sigma_{sr}^2} \tag{29}$$

where P_t is the power transmitted from the relay. For the dual-hop semi-blind relay scheme in the presence of interferers, the overall signal-to-interference plus noise ratio (SINR) at the destination node is given by [10]

$$\gamma = \frac{\gamma_1\gamma_2}{\gamma_2\gamma_I + \gamma_2 + C_1} \tag{30}$$

where $C_1 = \bar{\gamma}_1 + \bar{\gamma}_I N + 1$.

III. Performance Analysis

By utilizing the channel statistics obtained in the previous section, various important performance metrics of the mixed RF/FSO system are derived to analyze system performance.

A. Outage Probability

A communication system is in outage when the instantaneous end-to-end SNR falls below a specified threshold value γ_{th}, defined as $\Pr[\gamma < \gamma_{th}]$, where $\Pr[X]$ represents the probability of event X. For the considered system, the OP can be derived using the following relationship [10]

$$\begin{aligned} P_{out} &= P_r\left[\frac{\gamma_1\gamma_2}{\gamma_2\gamma_I + \gamma_2 + C_1} < \gamma_{th}|\gamma_2\right] \\ &= \int_0^\infty \int_0^\infty Pr\left[\gamma_1 < \gamma_{th}\left(\gamma_I + 1 + \frac{C_1}{\gamma_2}\right)\right] f_{\gamma_2}(\gamma_2) f_{\gamma_I}(\gamma_I) d\gamma_2 d\gamma_I \end{aligned} \tag{31}$$

Theorem 1: *The OP of an interference-limited mixed RF/FSO system with fixed-gain relaying in the presence of pointing errors over $\alpha-\mu$ atmospheric turbulence channels can be expressed as*

$$\begin{aligned} P_{out} = &\sum_{l=0}^{\mu_1-1} \mathcal{A}_1\Bigg[\mathcal{A}_2\Bigg[1 - e^{(-a_1\gamma_{th})}\sum_{m=0}^{\mu_1-l-1}\sum_{i=0}^{m}\sum_{j=0}^{i}\mathcal{A}_{6,1}(m,i,j) \\ &\times \gamma_{th}^{\,i+\frac{d}{2\rho}}\left[\frac{1}{\bar{\gamma}_I} + a_1\gamma_{th}\right]^{-(j+N)} \mathrm{G}_{0,g+h}^{g+h,0}\left[\mathcal{B}_{2,1}\gamma_{th}^{h}\middle|\begin{matrix}\cdot\\ \overline{k_1}\end{matrix}\right]\Bigg] + \mathcal{A}_3\Bigg[1- \\ &\times e^{(-a_2\gamma_{th})}\sum_{m=0}^{\mu_1-l-1}\sum_{i=0}^{m}\sum_{j=0}^{i}\mathcal{A}_{6,2}(m,i,j)\gamma_{th}^{\,i+\frac{d}{2\rho}}\left[\frac{1}{\bar{\gamma}_I} + a_1\gamma_{th}\right]^{-(j+N)} \\ &\times \mathrm{G}_{0,g+h}^{g+h,0}\left[\mathcal{B}_{2,2}\gamma_{th}^{h}\middle|\begin{matrix}\cdot\\ \overline{k_1}\end{matrix}\right]\Bigg]\Bigg] \end{aligned} \tag{32}$$

where G[.] is the Meijer-G function defined in [21, Eq. (9.301)], $\mathcal{A}_{6,k}(m,i,j) = \frac{\binom{m}{i}\binom{i}{j}C_1^{m-i}}{m!\bar{\gamma}_I^N(N-1)!}\mathcal{A}_{5,k}a_k$ with $\mathcal{A}_{5,k} = \mathcal{A}_4\frac{(g)^{\frac{1}{2}}(h)^{-(i-m+\frac{d}{2\rho}-\frac{1}{2})}}{(2\pi)^{\frac{h+g-2}{2}}}\left(C_1a_k\gamma_{th}\right)^{i-m+\frac{d}{2\rho}}$ and $k = 1, 2$. The ratio $\frac{h}{g} = \frac{\alpha}{\rho}$ determines the order of Meijer-G function, while the argument of Meijer-G function is derived to be $\mathcal{B}_{2,k} = \left(\frac{\mathcal{B}_1}{g}\right)^g\left(\frac{a_kC_1}{h}\right)^h$ and the parameters $k_1 = [\Delta(g,0), \quad \Delta(h, \frac{-d}{2\rho})]$ where $\Delta(k,a) = [a/k, (a+1)/k, \ldots, (a+k-1)/k]$, consists of $g+h$ terms.

Proof: The detailed proof can be found in Appendix B.

The outage analysis can be extended for the case of pointing errors with non-zero boresight, which has been presented in the following lemma.

Lemma 1: For the case of non-zero boresight pointing errors, the OP of the considered AF relaying system in the presence of interference can be expressed as

$$\begin{aligned} P_{out} = &\sum_{l=0}^{\mu_1-1}\mathcal{A}_1\Bigg[\mathcal{A}_2\Bigg(1 - e^{(-a_1\gamma_{th})}\sum_{m=0}^{\mu_1-l-1}\sum_{i=0}^{m}\sum_{j=0}^{i}\sum_{m_1=0}^{n}\Phi_7(m_1) \\ &\times \frac{\partial^{m_1}}{\partial s^{m_1}}\Bigg\{\Phi_{8,1}(s)\gamma^{\frac{\alpha\mu_2+\alpha s}{\rho}-1}\gamma_{th}^{\,b_1}\left[\frac{1}{\bar{\gamma}_I} + a_1\gamma_{th}\right]^{-(j+N)} \\ &\times \mathrm{G}_{g,2g+h}^{2g+h,0}\left[\Phi_{9,1}\gamma_{th}^{h}\middle|\begin{matrix}\Phi_{10}\\ \Phi_{11}\end{matrix}\right]\Bigg\}\Bigg) + \mathcal{A}_3\Bigg(1 - e^{(-a_2\gamma_{th})}\sum_{m=0}^{\mu_1-l-1}\sum_{i=0}^{m}\sum_{j=0}^{i} \\ &\times \sum_{m_1=1}^{n}\Phi_7(m_1)\frac{\partial^{m_1}}{\partial s^{m_1}}\Bigg\{\Phi_{8,2}(s)\gamma^{b_1}\left[\frac{1}{\bar{\gamma}_I} + a_1\gamma_{th}\right]^{-(j+N)} \\ &\times \mathrm{G}_{g,2g+h}^{2g+h,0}\left[\Phi_{9,2}\gamma_{th}^{h}\middle|\begin{matrix}\Phi_{10}\\ \Phi_{11}\end{matrix}\right]\Bigg\}\Bigg)\Bigg] \end{aligned} \tag{33}$$

where $b_1 = (\alpha\mu_2 + \alpha s)/\rho + i - m_1$, $\Phi_7(m_1) = \frac{\Gamma(N+j)\binom{j}{i}\Phi_1(m_1)}{\bar{\gamma}_I^N(N-1)!}$, $\Phi_{8,k}(s) = (a_kC_1)^{b_1}\frac{g^{-s-1/2h-b_1-1/2}}{(2\pi)^{(g+h-2)/2}}$, the involved parameters can be defined as $\Phi_{10} = [\Delta(g,1)]$, $\Phi_{11} = [\Delta(g,-s), \Delta(g,0), \Delta(h,-b_1)]$ while the argument of the Meijer-G is derived as $\Phi_{9,k} = (\Phi_3/g)^g(C_1a_k/h)^h$.

Proof: Substituting CDF of RF link from (5) and the PDF for instantaneous SNR for non-zero boresight pointing error from (22) into (31), and applying identity [28, Eq. (07.34.21.0013.01)], the expression for OP presented in (33) can be derived.

Lemma 2: The approximate OP of the considered mixed

RF/FSO relaying system with non-zero boresight pointing error can be expressed as

$$P_{out} \simeq \Phi_5 \sum_{m_2=0}^{J} \Phi_6(m_2) \sum_{l=0}^{\mu_1-1} \mathcal{A}_1 \Bigg[\mathcal{A}_2 \Bigg\{ 1 - e^{(-a_1\gamma_{th})} \sum_{m=0}^{\mu_1-l-1} \sum_{i=0}^{m} \times \sum_{j=0}^{i} \frac{\binom{m}{i}\binom{i}{j} {C_1}^{m-i}}{\bar{\gamma}_I^N (N-1)!} \Gamma(m-i-b_2) \left[\frac{1}{\bar{\gamma}_I} + a_1\gamma_{th} \right]^{-(j+N)} \times (a_1 C_1 \gamma_{th})^{i-m-b_2} \Bigg\} + \mathcal{A}_3 \Bigg\{ 1 - e^{(-a_2\gamma_{th})} \sum_{m=0}^{\mu_1-l-1} \sum_{i=0}^{m} \sum_{j=0}^{i} \times \frac{\binom{m}{i}\binom{i}{j} {C_1}^{m-i}}{\bar{\gamma}_I^N (N-1)!} \Gamma(m-i-b_2) \left[\frac{1}{\bar{\gamma}_I} + a_2\gamma_{th} \right]^{-(j+N)} \times (a_2 C_1 \gamma_{th})^{i-m-b_2} \Bigg\} \Bigg] \tag{34}$$

where $b_2 = \frac{\alpha\mu_2 + \alpha m_2}{\rho}$.

Proof: By using the approximate PDF on FSO link with non-zero boresight errors in (26) into the definition of P_{out} in (31), and on performing some mathematical manipulations, the expression in (34) can be derived.

It is more useful to find an asymptotic representation for the exact analysis to obtain quick insights into the overall performance of system for the case when SNR increases. Next, the asymptotic approximation of the end-to-end OP for the case for non-zero boresight pointing error is presented for further study.

Lemma 3: The asymptotic expression for the OP for the considered mixed RF/FSO system over $\alpha - \mu$ turbulence channels with non-zero pointing errors can be expressed as

$$P_{out} \simeq \sum_{l=0}^{\mu_1-1} \mathcal{A}_1 \Bigg[\mathcal{A}_2 \Bigg(1 - e^{(-a_1\gamma_{th})} \sum_{m=0}^{\mu_1-l-1} \sum_{i=0}^{m} \sum_{j=0}^{i} \sum_{m_1=0}^{n} \Phi_7(m_1) \times \frac{\partial^{m_1}}{\partial s^{m_1}} \Bigg\{ \Phi_{8,1}(s) \gamma^{\frac{\alpha\mu_2+\alpha s}{\rho}-1} \gamma_{th}^{b_1} \left[\frac{1}{\bar{\gamma}_I} + a_1\gamma_{th} \right]^{-(j+N)} \times \sum_{j_1=1}^{2g+h} \frac{\prod_{j_2=1, j_2\neq j_1}^{2g+h} \Gamma\left(\Phi_{11,j_2} - \Phi_{11,j_1}\right)}{\Gamma\left(\Phi_{10,j_2} - \Phi_{11,j_1}\right)} \left(\Phi_{9,1}\gamma_{th}^{h}\right)^{\Phi_{11,j_1}} \Bigg\} \Bigg) + \mathcal{A}_3 \Bigg(1 - e^{(-a_2\gamma_{th})} \sum_{m=0}^{\mu_1-l-1} \sum_{i=0}^{m} \sum_{j=0}^{i} \sum_{m_1=0}^{n} \Phi_7(m_1) \frac{\partial^{m_1}}{\partial s^{m_1}} \Bigg\{ \Phi_{8,2}(s) \times \gamma_{th}^{b_1} \left[\frac{1}{\bar{\gamma}_I} + a_1\gamma_{th} \right]^{-(j+N)} \sum_{j_1=1}^{2g+h} \frac{\prod_{j_2=1, j_2\neq j_1}^{2g+h}}{\Gamma\left(\Phi_{10,j_2} - \Phi_{11,j_1}\right)} \times \Gamma\left(\Phi_{11,j_2} - \Phi_{11,j_1}\right) \left(\Phi_{9,2}\gamma_{th}^{h}\right)^{\Phi_{11,j_1}} \Bigg\} \Bigg) \Bigg] \tag{35}$$

Proof: For asymptotic analysis, as $\Psi_\rho \to \infty$, the value of $\Phi_{9,k}$ diminishes, i.e., $\Phi_{9,k} \to 0$. Further to this, the Meijer-G function can be approximated for small arguments with the aid of [28, Eq. (07.34.06.0006.01)] to obtain (35).

B. Coding Gain and Diversity Order Analysis

The exact analysis of OP fails in providing quick insights into various system parameters from a designer's perspective. The exact analysis of error probabilities (OP or BER) can be modified for the case of large SNR which allows one to gain information about the main factors that determine the performance of the wireless optical link. In the subsequent discussions, an analytical framework is developed to evaluate parameters affecting system performance in terms of diversity order and coding gain.

The diversity order G_d is conventionally defined as the negative asymptotic slope of the outage performance versus SNR on a log scale [29]. On the other hand, coding gain G_c provides the amount of shift in the SNR on the outage curve relative to the reference curve of $(\bar{\gamma}_1)^{-G_d}$. Notably, the exact results of OP can be approximated in the high SNR regime given by the relation [30] $P_{out} \simeq \left(G_c \bar{\gamma}_1\right)^{-G_d}$.

Theorem 2: *The diversity order G_d and the coding gain G_c of a mixed RF/FSO fixed gain relaying scheme in the presence of multiple interferers is given by*

$$G_d = \alpha(p_0 - 1) + 1 \tag{36}$$

and

$$G_c = \left[\Lambda_1 \Lambda_2 \kappa^{-\alpha(p_0-1)} \right]^{\frac{1}{\alpha[p_0-1]+1}} \tag{37}$$

where $p_0 = \frac{d-2\rho}{\alpha\rho}$, κ is defined by the relation $\bar{\Psi}_\rho = \kappa\bar{\gamma}_1$, while Λ_1 and Λ_2 are expressed as

$$\Lambda_1 = \sum_{l=0}^{\mu_1-1} 2\mathcal{A}_1[\mu_1(h-H)\mathcal{A}_2 + \mu_1(h+H)\mathcal{A}_2] \tag{38}$$

$$\Lambda_2 = \frac{\xi^2 2^{p_0+1} C_1 \gamma_{th} \Gamma(p_0) \mu_2^{\frac{d}{2}-p_0} \{\mathbb{E}[\mathrm{I}_a]\}^{-p_0\alpha-\alpha}}{\alpha\rho\Gamma(\mu_2)(A_o\hat{\omega}_a)^{-p_0\alpha-\frac{d}{2}} I_l^{\frac{d}{2}}} \times W_{\frac{\alpha\mu_2-\xi^2-\alpha}{2\alpha}, \frac{\xi^2-\alpha\mu_2}{2\alpha}} \left(\frac{\mu_2}{\hat{\omega}_a^\alpha} \right) I_l^{\frac{d}{2}-1} \tag{39}$$

Proof: The proof is provided in Appendix C.

The diversity order G_d of the relay-aided transmission depends upon fading parameters α, μ_2, and the type of demodulation ρ. It is interesting to note that G_d does not depend upon the RF link parameters and is controlled by the wireless optical link transmission characteristics. From the coding gain G_c developed in (37), it can be considered that the coding depends upon RF and optical link of the dual hop AF relay scheme. It is notable that G_d and G_c do not depend on the interferer characteristics and even with uncoded transmission the coding gain can be obtained in favorable atmospheric conditions with minimum pointing errors.

C. Bit Error Rate

The authors in [31] have presented an interesting formula for the average BER for a variety of modulation schemes as

$$\bar{P}_b = \frac{q^p}{2\Gamma(p)} \int_0^\infty \gamma^{p-1} \exp(-q\gamma) F(\gamma) d\gamma \tag{40}$$

where the combinations of the parameters p and q define the modulation schemes. An extensive list of binary modulation schemes defined by combinations of parameters p and q is provided in [31].

Theorem 3: *The average BER of a mixed RF/FSO fixed gain relaying scheme in the presence of multiple interferers is given by*

$$\bar{P}_b = \sum_{l=0}^{\mu_1-1} \mathcal{A}_1 \left[\mathcal{A}_2 \left\{ \frac{1}{2} - \sum_{m=0}^{\mu_1-l-1} \sum_{i=0}^{m} \sum_{j=0}^{i} \mathcal{A}_{7,1}(m,i,j) \mathcal{H}_1(a_1, \mathcal{B}_{2,1}) \right\} + \mathcal{A}_3 \left\{ \frac{1}{2} - \sum_{m=0}^{\mu_1-l-1} \sum_{i=0}^{m} \sum_{j=0}^{i} \mathcal{A}_{7,2}(m,i,j) \mathcal{H}_1(a_2, \mathcal{B}_{2,2}) \right\} \right] \tag{41}$$

where

$$\mathcal{H}_1(a_k, \mathcal{B}_{2,k}) = H_{\mathbf{x}_1}^{\mathbf{x}_2} \left(\begin{array}{c|c|c} (k_2;1;h) & (k_3,1) & \text{—} \\ \text{—} & (0,1) & (\mathrm{k}_1,1) \end{array} \middle| \mathcal{Z}_{1,k}, \mathcal{Z}_{2,k} \right)$$

with $H_{x_1,x_2:x_3,x_4:x_5,x_6}^{0,y_2:y_3,y_4:y_5,y_6}(.)$ is bivariate H-function defined in [32, Eq. (2.1)]. The parameters k_2 and k_3 are derived to be $k_2 = 1 - p - \frac{d}{2\rho}$, $k_3 = 1 - N - j$, while the constants involved are defined as: $\mathcal{A}_{7,k}(m,i,j) = \mathcal{A}_{6,k} \frac{q^p}{\Gamma(p)} \left(q + a_k\right)^{-(i+\frac{d}{2\rho}+1)}$. We define the order of Fox-H function as $\{\mathbf{x}_1, \mathbf{x}_2\} = \{(0,1:1,1:\text{g+h},0),(1,0:1,1:0,\text{g+h})\}$. Moreover, the arguments of bivariate H-function involved in (41) can be expressed as: $\mathcal{Z}_{1,k} = \frac{a_k \bar{\gamma}_I}{q+a_k}$, $\mathcal{Z}_{2,k} = \frac{\mathcal{B}_{2,k}}{(q+a_k)^h}$.

Proof: See Appendix D.

Efficient MATHEMATICA software implementation of bivariate Meijer-G function has been provided in [31] which can be utilized to develop a computationally efficient algorithm to compute bivariate Fox-H function. The author in [33] has reported a MATLAB code for evaluation of Fox's-H function of two variables.

In order to analyze the BER performance of the proposed system model in the presence of non-zero boresight component of pointing error, a BER expression has been derived for the case of non-zero boresight through the following lemma:

Lemma 4: The approximate BER of the considered mixed RF/FSO relaying system with non-zero boresight pointing error can be expressed as

$$P_b \simeq \Phi_5 \sum_{m_2=0}^{J} \Phi_6(m_2) \sum_{l=0}^{\mu_1-1} \mathcal{A}_1 \left[\mathcal{A}_2 \left\{ \frac{1}{2} - \sum_{m=0}^{\mu_1-l-1} \sum_{i=0}^{m} \sum_{j=0}^{i} \times \frac{\bar{\gamma}_I^j q^p \binom{m}{i} \binom{i}{j} {C_1}^{m-i}}{2\Gamma(p)(N-1)!} \Gamma(m-i-b_2)(a_1 C_1)^{i-m-b_2} \times \mathrm{G}_{2,1}^{1,2} \left[\frac{a_1 \bar{\gamma}_I}{q+a_1} \middle| \begin{matrix} 1-(p+i-m-b_2), 1-j-N \\ 0 \end{matrix} \right] \right\} + \mathcal{A}_3 \left\{ \frac{1}{2} - \times \sum_{m=0}^{\mu_1-l-1} \sum_{i=0}^{m} \sum_{j=0}^{i} \frac{\bar{\gamma}_I^j q^p \binom{m}{i} \binom{i}{j} {C_1}^{m-i}}{2\Gamma(p)(N-1)!} \Gamma(m-i-b_2) \times (a_2 C_1)^{i-m-b_2} \mathrm{G}_{2,1}^{1,2} \left[\frac{a_2 \bar{\gamma}_I}{q+a_2} \middle| \begin{matrix} 1-(p+i-m-b_2), 1-j-N \\ 0 \end{matrix} \right] \right\} \right] \tag{42}$$

Proof: Substituting γ_{th} by γ in (34) and using (40), the BER for non-zero boresight pointing error can be formulated as in (40). To this end, with the aid of [28, Eq. (07.34.21.0088.01)], a closed-form expression for the BER in the presence of non-zero boresight pointing error can be derived.

Moreover, similar to OP, the high SNR approximation of BER can be determined to gain better insights about the error performance of relaying strategy. For this, we resort to Mellin-Barnes integral representation of $\mathcal{H}_1(a_k, \mathcal{B}_{2,k})$ as per [32, Eq. (2.1)]. According to residue theorem [34, Theorem 1.7 and Theorem 1.11], Fox-H function can be approximated as asymptotic expansions by evaluating the residue of the Mellin-Barnes integral at the poles closest to the contour of integration. The bivariate Fox-H function involved in 41 can be represented in Mellin-Barnes integral form using [32, Eq. (2.1)] as

$$\mathcal{H}_1(a_k, \mathcal{B}_{2,k}) \underset{\bar{\Psi}_\rho \gg 1}{\simeq} \frac{1}{(2\pi i)^2} \int_{\mathcal{L}_1} \int_{\mathcal{L}_2} \Gamma(1+i+\frac{d}{2\rho} - z_1 - h z_2) \times \Gamma(z_1)\Gamma(N+j-z_1) \prod_{j_1=1}^{g+h} \Gamma(k_{1,j_1} - z_2) {\mathcal{Z}_{1,k}}^{-z_1} {\mathcal{Z}_{2,k}}^{-z_2} \tag{43}$$

The complex integral over the contour $\mathcal{L}_1$ can be represented as Fox-H function with the aid of [34, Eq. (1.2)] and further expressed in terms if Gauss-hypergeometric function using [34, Eq. (1.131)]. In addition to this, assuming that β is the pole closest to the contour of integration, given as $\beta = \min(k_1)$, and noting the fact that as $\Psi_\rho \to \infty$, we have $\mathcal{Z}_{2,k} \to 0$. For small arguments, calculating the residue at the pole lying to the right of the contour, the asymptotic representation of 41 can be given as

$$\mathcal{H}_1(a_k, \mathcal{B}_{2,k}) \underset{\bar{\Psi}_\rho \gg 1}{\simeq} \Gamma(N+j) {}_2F_0(1+i+\frac{d}{2\rho} - h\beta, N+j;;-\mathcal{Z}_{1,k}) \times \Gamma\left(1+i+\frac{d}{2\rho} - h\beta\right) \Gamma(N+j-z_1) \prod_{j_1=1}^{g+h} \Gamma(k_{1,j_1} - \beta) {\mathcal{Z}_{2,k}}^{-\beta} \tag{44}$$

where ${}_pF_q(.)$ is the Gauss-hypergeometric function as defined in [21, Eq. (9.111.1)].

D. Ergodic Capacity

Yet another important performance metric of the relay-assisted communication system is the capacity offered when limited by noisy channel for reliable transmission. The ergodic capacity is given as [35]

$$\bar{C} = \frac{1}{\ln(2)} \int_0^\infty \log_2(1+\delta\gamma) f(\gamma) d\gamma \tag{45}$$

where $\delta = \frac{e}{2\pi}$ [36] for IM/DD reception technique and $\delta = 1$ for coherent detection, while $f(\gamma)$ represents the end-to-end PDF of the dual hop AF relay system. It is noteworthy that (45) provides a lower bound on the ergodic capacity for IM/DD detection technique. In order to make use of (45) in order to evaluate the capacity offered, the end-to-end PDF of instantaneous SNR is required. By following the procedure as illustrated in Appendix E, the PDF of the considered system is derived in (46). Moreover, in (46), $p_1 = \frac{d}{2\rho} - \mu_1 + l + r + 1$, $k_4 = [\Delta(g,0), \quad \Delta(h,-p_1)]$, $k_5 = [\Delta(g,0), \quad \Delta(h,1-p_1)]$. The constants $\mathcal{A}_{8,k}$ and $\mathcal{A}_{9,k}$ are derived as $\mathcal{A}_{8,k} = {C_1}^{\frac{d}{2\rho}} \mathcal{A}_4 {a_k}^{p_1} \frac{\sqrt{g}(h)^{-p_1-0.5}}{(2\pi)^{\frac{g+h-2}{2}}}$ and $\mathcal{A}_{9,k} = {C_1}^{\frac{d}{2\rho}-1} \mathcal{A}_4 {a_k}^{p_1-1} \frac{\sqrt{g}(h)^{-p_1+0.5}}{(2\pi)^{\frac{g+h-2}{2}}}$. Plugging the PDF in (45), we derive the ergodic capacity expression in the next theorem.

$$f(y)=\sum_{l=0}^{\mu_1-1}\mathcal{A}_1 y^{\mu_1-l-1}\sum_{r=0}^{\mu_1-l-1}\binom{\mu_1-l-1}{r}\Bigg[(-1)^l\Bigg\{\frac{e^{-a_1 y}y^{p_1}}{\bar{\gamma}_I{}^N(N-1)!}[a_1y+\frac{1}{\gamma_I}]^{-N}\Bigg(\sum_{s_1=0}^{r+1}\binom{r+1}{s_1}\Gamma(s_1+N)\mathcal{A}_{8,1}\mathrm{G}_{0,g+h}^{g+h,0}\left[\mathcal{B}_{2,1}y^h\middle|\begin{matrix}\\ \overline{k_4}\end{matrix}\right]$$
$$\times[a_1y+\frac{1}{\gamma_I}]^{-s_1}+\sum_{s_2=0}^{r}\binom{r}{s_2}\Gamma(s_2+N)\mathcal{A}_{9,1}y^{-1}[a_1y+\frac{1}{\gamma_I}]^{-s_2}\mathrm{G}_{0,g+h}^{g+h,0}\left[\mathcal{B}_{2,1}y^h\middle|\begin{matrix}\\ \overline{k_5}\end{matrix}\right]\Bigg)\Bigg\}+(-1)^{\mu_1}\Bigg\{\frac{e^{-a_2y}y^{p_1}}{\bar{\gamma}_I{}^N(N-1)!}[a_2y+\frac{1}{\gamma_I}]^{-N}\Bigg(\sum_{s_1=0}^{r+1}$$
$$\times\binom{r+1}{s_1}\Gamma(s_1+N)\mathcal{A}_{8,2}[a_2y+\frac{1}{\gamma_I}]^{-s_1}\mathrm{G}_{0,g+h}^{g+h,0}\left[\mathcal{B}_{2,2}y^h\middle|\begin{matrix}\\ \overline{k_4}\end{matrix}\right]+\sum_{s_2=0}^{r}\binom{r}{s_2}\Gamma(s_2+N)\mathcal{A}_{9,2}y^{-1}[a_2y+\frac{1}{\gamma_I}]^{-s_2}\mathrm{G}_{0,g+h}^{g+h,0}\left[\mathcal{B}_{2,2}y^h\middle|\begin{matrix}\\ \overline{k_5}\end{matrix}\right]\Bigg)\Bigg\}\Bigg] \tag{46}$$

$$\bar{C}=\sum_{l=0}^{\mu_1-1}\frac{\mathcal{A}_1}{\ln(2)}\sum_{r=0}^{\mu_1-l-1}\frac{\binom{\mu_1-l-1}{r}}{\bar{\gamma}_I{}^N(N-1)!}\Bigg[(-1)^l\Bigg\{\Bigg(\sum_{s_1=0}^{r+1}\binom{r+1}{s_1}\Gamma(s_1+N)[\frac{1}{\gamma_I}]^{-s_1-N}\mathcal{A}_{8,1}\mathcal{J}_{1,1}+\sum_{s_2=0}^{r}\binom{r}{s_2}\Gamma(s_2+N)\mathcal{A}_{9,1}\mathcal{J}_{2,1}\Bigg)\Bigg\}$$
$$+(-\mu_1)^l\Bigg\{\Bigg(\sum_{s_1=0}^{r+1}\binom{r+1}{s_1}\Gamma(s_1+N)[\frac{1}{\gamma_I}]^{-s_1-N}\mathcal{A}_{8,2}\mathcal{J}_{1,2}+\sum_{s_2=0}^{r}\binom{r}{s_2}\Gamma(s_2+N)\mathcal{A}_{9,2}\mathcal{J}_{2,2}\Bigg)\Bigg\}\Bigg] \tag{47}$$

$$\mathcal{J}_{1,k}=\frac{(a_k)^{-p_1+\mu_1-l}}{\Gamma(s_1+N)}H_{\mathbf{x}_4}^{\mathbf{x}_3}\left(\begin{matrix}1-p_1-\mu_1+l;1,1,h\\ \_\_\_\_\_\end{matrix}\middle|\begin{matrix}(0,1)\\(0,1)\end{matrix}\middle|\begin{matrix}(1-N,1)\\(0,1)\end{matrix}\middle|\begin{matrix}\_\_\_\_\_\\(k_1,[1]_{\mathrm{length}(k_1)})\end{matrix}\middle|\delta\bar{\gamma}_I,\bar{\gamma}_I,B_1\bar{\gamma}_1{}^h\right) \tag{48}$$

$$\mathcal{J}_{2,k}=\frac{(a_k)^{-p_1+\mu_1-l}}{\Gamma(s_2+N)}H_{\mathbf{x}_4}^{\mathbf{x}_3}\left(\begin{matrix}2-p_1-\mu_1+l;1,1,h\\ \_\_\_\_\_\end{matrix}\middle|\begin{matrix}(0,1)\\(0,1)\end{matrix}\middle|\begin{matrix}(1-N,1)\\(0,1)\end{matrix}\middle|\begin{matrix}\_\_\_\_\_\\(k_1,[1]_{\mathrm{length}(k_1)})\end{matrix}\middle|\delta\bar{\gamma}_I,\bar{\gamma}_I,B_1\bar{\gamma}_1{}^h\right) \tag{49}$$

Theorem 4: *The ergodic capacity of the dual-hop mixed RF/FSO AF relaying system in the presence of interference can be expressed as given in (47).*

In (48) and (32) $H_{x_1,x_2:x_3,x_4:x_5,x_6:x_7,x_8}^{0,y_2:y_3,y_4:y_5,y_6:y_7,y_8}(.)$ denotes the trivariate H-function as defined in [37] as an extension to H-function of two variables. The parameter array k_1 is of length $g+h$ and $[1]_{\mathrm{length}(k_1)}$ represents an array of 1's of length equal to that of k_1. The order of Fox-H function is defined as $\{\mathbf{x}_3,\mathbf{x}_4\}=\{(0,1:1,1:1,2:\mathrm{g+h},0),(1,0:1,1:2,2:0,\mathrm{g+h})\}$. The implementation of the multivariate H-function can be done using the Python code provided in [38].

Proof: The proof of Theorem 4 is provided in Appendix F.

Furthermore, in order to relate with the capacity results quickly, the asymptotic analysis for the same needs to be addressed. Following the procedure developed in Appendix F, the asymptotic approximate expression of the trivariate Fox-H function in (48) and (32) for high SNR regime can be derived as given below:

$$\mathcal{J}_{1,k}\underset{\bar{\Psi}_\rho,\bar{\gamma}_1\gg1}{\simeq}\sum_{j_1=1}^{g+h}\prod_{j_2=1,j_1\neq j_2}^{g+h}\bar{\gamma}_I{}^{s_1+N}a_k{}^{-p_2}\frac{\Gamma(1+\beta)\Gamma^2(-\beta)}{\Gamma(1+x)}\left(\frac{\delta}{a_k}\right)^{-\beta}$$
$$\times\Gamma(p_2-\beta)_2F_0(p_2-\beta,s_1+N;;-\bar{\gamma}_I) \tag{50}$$

$$\mathcal{J}_{2,k}\underset{\bar{\Psi}_\rho,\bar{\gamma}_1\gg1}{\simeq}\sum_{j_1=1}^{g+h}\prod_{j_2=1,j_1\neq j_2}^{g+h}\bar{\gamma}_I{}^{s_2+N}a_k{}^{-(p_2-1)}\frac{\Gamma(1+\beta)\Gamma^2(-\beta)}{\Gamma(1+x)}$$
$$\times\left(\frac{\delta}{a_k}\right)^{-\beta}\Gamma(p_2-1-\beta)_2F_0(p_2-1-\beta,s_2+N;;-\bar{\gamma}_I) \tag{51}$$

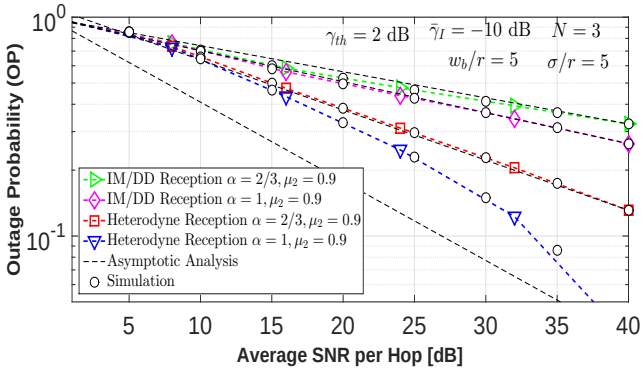

Fig. 2. Outage probability for IM/DD and coherent detection schemes over $\alpha-\mu$ turbulence channel with pointing error parameters fixed at $w_b/r=5$ and $\sigma/r=4$, $\gamma_{th}=2$ dB, N=3 and different levels of turbulence.

where $p_2=p_1+\mu_1-l+hk_{1,j_1}$. Furthermore, after placing (50) and (51), in (47), we get the asymptotic expression for the ergodic capacity of the proposed network.

It is noteworthy that compared to exact analysis in (47), the asymptotic approximated expression in (50) and (51) yield much quicker insights into the throughput offered by the relaying system. With all the elementary functions, (50) and (51) provide information about key factors affecting the system explicitly. Since the term β is dominated by $\min(k_1)$, the capacity of overall relay scheme is determined by few terms in the summation.

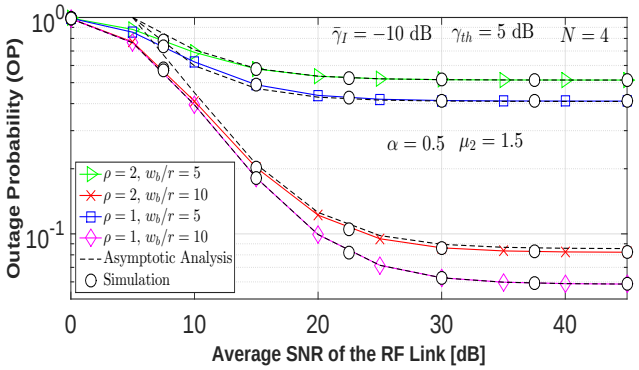

Fig. 3. Impact of pointing error on outage probability vs average SNR of the RF link for both kinds of detection schemes. Electrical SNR is fixed at 30 dB and system is subjected to N=4 interferers each with $\gamma_I = -10$ dB.

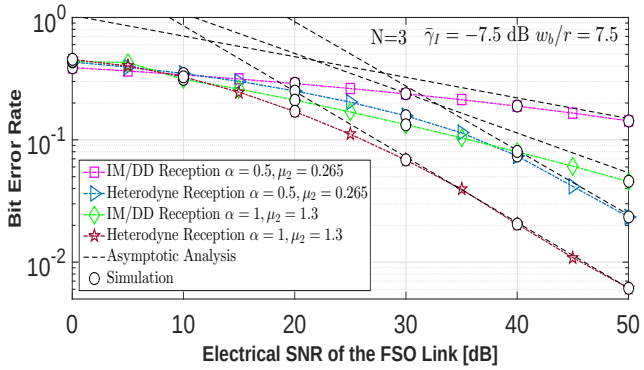

Fig. 6. Analysis of BER vs average electrical SNR over $\alpha - \mu$ fading channel by varying the turbulence conditions with pointing error parameters fixed at $w_b/r = 7$ and $\sigma/r = 5$.

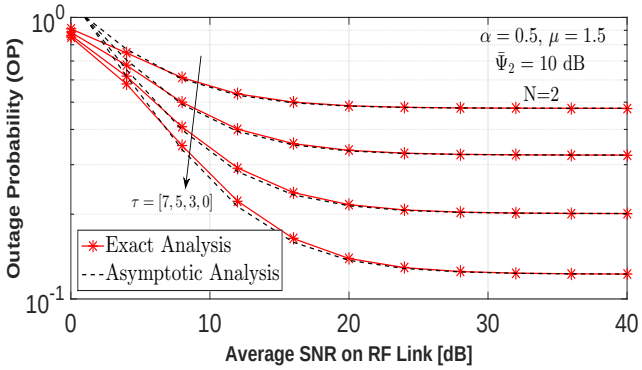

Fig. 4. Analysis of outage probability vs average SNR by varying the strength of pointing error with non-zero boresight parameters fixed at $w_b/r = 4$, $N = 2$ and RF SNR threshold $\gamma_{th} = 1$ dB.

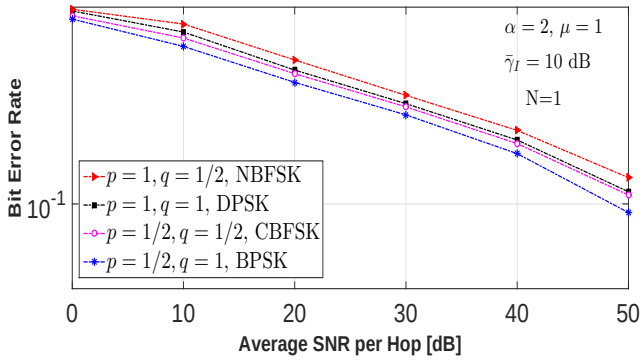

Fig. 7. Comparison of BER performance of binary modulation schemes of IM/DD receiver system over $\alpha - \mu$ fading channel with interference strength of $\bar{\gamma}_I = 10$ dB.

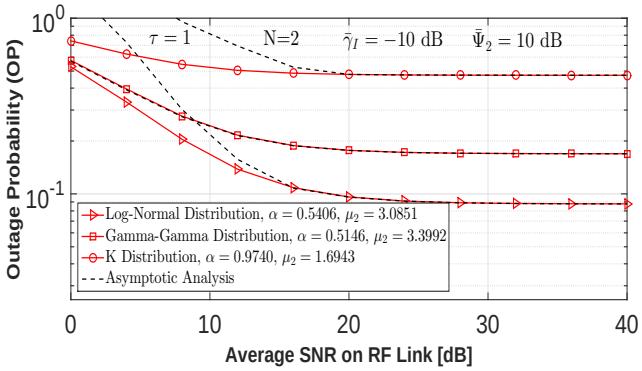

Fig. 5. Outage probability vs average SNR on RF link for existing FSO channel models using $\alpha - \mu$ distribution.

IV. Numerical Results and Discussion

In this section, we have presented the numerical examples corresponding to analytical frame work developed in this paper. OP, BER and capacity dependency on various factors such as number of interferers and average SNR is illustrated in various plots. The choice of model parameters is kept arbitrary to prove the validity of the obtained results. The numerical results obtained in the present work are validated by computer-based simulations in MATLAB software. We have considered $h - H = 0.5$ and $h/H = 1$, to demonstrate various characteristic plots in this section.

In Fig. 2, we illustrate the OP variations of mixed RF/FSO relay system experiencing different strength of turbulence for IM/DD and heterodyne detection schemes. We fix the number of interferers $N = 3$, each with average power $\bar{\gamma}_I = -10$ dB. It can be observed that the heterodyne detection reduces the outage experienced by the FSO link. We also demonstrate the high SNR approximation in the same plot and it can be observed from Fig. 2 that the asymptotic results converge with the exact results as the value of average SNR increases. As expected, it is evident from the plot that as the average SNR (per hop) is increased, the OP decreases implying better reliability of communication system.

Fig. 3 depicts the OP for $\alpha = 0.5$ and $\mu_2 = 1.5$ as a function of average SNR on the RF link for different values of pointing error. In this plot, we consider both types of detection schemes. The electrical SNR on the FSO link is kept constant at 30 dB in the plot with threshold of γ_{th} of 5 dB. Since, the amount of misalignment between transmitter and receiver telescopes is inversely proportional to the value of ratio $\frac{w_b}{r}$ therefore, decrease in this ratio presents more diverse effect on the FSO link of the dual hop scheme in terms of pointing error. We can conclude that increase in pointing error decreases the reliability of the overall system. It can be observed that as the average

SNR on the RF link is increased, the OP curve saturates and no further change takes place. In Fig. 4, the OP is plotted against the average SNR on the RF link for varying strength of boresight pointing error. Turbulence experienced by the FSO link is modeled as $\alpha = 0.5$ and $\mu_2 = 1.5$. The threshold SNR is kept at $\gamma_{th} = 1$ dB, whereas the average INR is assumed to be $\bar{\gamma}_I = -10$ dB. Specifically, in Fig. 4, the effect of non-boresight pointing errors can be observed as performance of dual hop scheme improves when the value of τ reduces. Notably, as $\tau \to 0$, the PDF in (17) reduces to the case of zero-boresight pointing errors. Moreover, the asymptotic representation matches with the results as the average SNR on the RF link increases. In Fig. 5, the generalization capability of the α-μ distribution has been illustrated. To represent weak-to-moderate-to-strong turbulence conditions, the model parameters for the α-μ distribution have been estimated by evaluating (14) and (15) for log-normal, Gamma-Gamma and K-distributions. After solving the system of equations numerically, the values of model parameters have been evaluated as $(\alpha, \mu_2) = (0.5406, 3.08.15)$ for log-normal, $(0.5146, 3.3992)$ for Gamma-Gamma and $(0.9740, 1.6943)$ for K-distribution. The boresight error component in the plot has been assumed to be $\tau = 1$ and number of interferers has been fixed to $N = 2$. It can be noted that the $\alpha - \mu$ distribution has the capability to model weak-to-moderate-to-strong turbulence conditions on the FSO link.

In Fig. 6, we present BER performance for both types of detection schemes. We consider, $p = 0.5$ and $q = 1$ in the plot, which corresponds to BPSK modulation scheme. For fixed $\bar{\gamma}_I$ of -7.5 dB at $(\alpha, \mu_2) = (1/2, 0.265)$ and $(1, 1.3)$, it can be concluded from the plot that as the average electrical SNR on the FSO link increases, the BER decreases. The asymptotic results obtained in the present work follow with the theoretical analysis saving the complexity of evaluating bivariate Fox's H function. Next, the comparison of binary modulation schemes on the BER performance of a IM/DD based receiver can be studied from Fig. 7. In this plot, BER is minimum for BPSK (when $p = 1/2, q = 1$) when the FSO link undergoes moderate turbulence with model parameters $(\alpha, \mu_2) = (2, 1)$. The performance of differential phase shift keying (DPSK) (obtained by setting $p = q = 1$), coherent binary frequency shift keying (CBFSK) (when $p = q = 1/2$), and non-coherent FSK (NFSK) can be compared. The interference level has been set to $\bar{\gamma}_{th} = -10$ dB.

The variation in BER performance with increment in number of interferers for both kinds of detection schemes is presented in Fig. 8. It is noteworthy that the coherent demodulation mechanism performs better than direct detection based receiver system. Fig. 8 also demonstrates the impact of increasing the average SNR on the RF link. For $\bar{\gamma}_1 = 10$ dB, a comparison of $N = 2$ and $N = 3$ is performed corresponding to both the detection schemes. It is apparent from the plot that at $N = 2$ interferers, BER performance is better as compared to when the number of interferer is $N = 3$. Furthermore, when the average SNR on the RF hop is decreased to $\bar{\gamma}_1 = 5$ dB with $N = 2$ interferers, the BER performance deteriorates. In order to emphasize on the generalization capability of the $\alpha - \mu$ model, the effect of multiple CCIs and non-zero boresight error has been demonstrated in Fig. 9. Weak turbulence conditions is modeled using the log-normal distribution, while moderate and strong turbulence using Gamma-Gamma and K-distribution, respectively. The variation of turbulence conditions have been characterized using the $\alpha - \mu$ model by estimating the model parameters using the relationships (14) and (15).

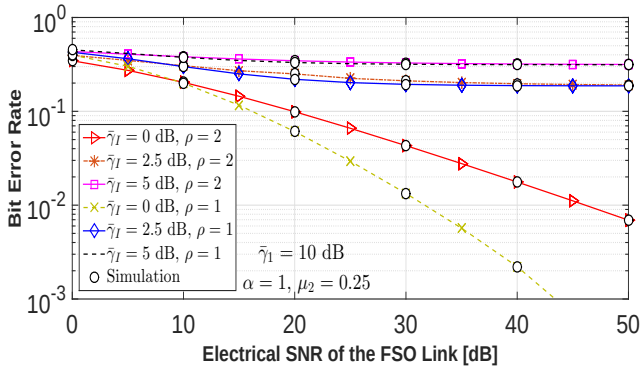

Fig. 8. BER vs electrical SNR of the FSO link over $\alpha - \mu$ turbulence channel by varying numbers interferers on the relay node with pointing error parameters fixed at $w_b/r = 10$ and $\sigma/r = 5$.

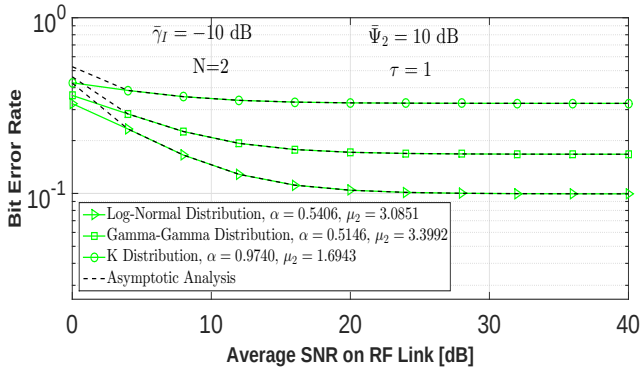

Fig. 9. BER vs average SNR on RF link for existing FSO channel models using $\alpha - \mu$ distribution.

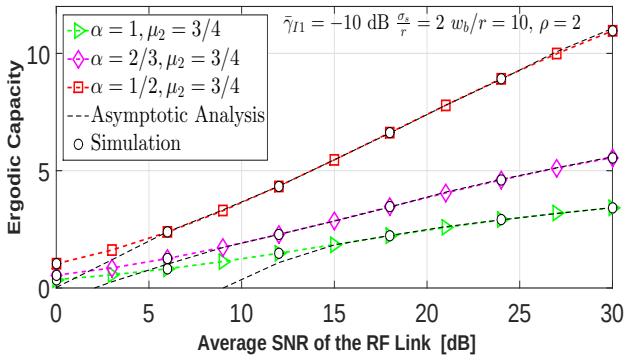

Fig. 10. Ergodic capacity vs average SNR of the RF link over $\alpha - \mu$ turbulence channel for different combinations of model parameters with pointing error parameters fixed at $w_b/r = 10$ and $\sigma/r = 2$.

Ergodic capacity analytical and simulation results are shown in Fig. 10 and Fig. 11. Specifically, for $(\alpha, \mu_2) = (0.5, 0.75), (0.66, 0.75), (1, 0.75)$, Fig. 10 presents ergodic capacity verses average SNR on RF link plot in the presence of $N = 2$ interferers with fixed average SINR of -10 dB.

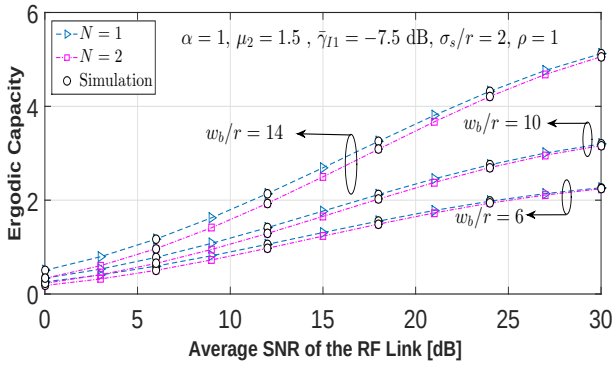

Fig. 11. Analysis of ergodic capacity vs average SNR of the RF link over $\alpha - \mu$ turbulence channel by varying the number of interferers effecting the system with pointing error parameters fixed at $w_b/r = 7$ and $\sigma/r = 4$.

We consider both types of detection schemes in this plot. As clear from the plot, the increase in $\bar{\Psi}_\rho$ on the FSO link increases the capacity offered by the system. We also present the asymptotic high electrical SNR in Fig. 10 and it is evident that the approximation follows closely with the exact analytical results.

In Fig. 11, we show the effect of varying the number of interferers, with different levels of pointing errors on the capacity verses average SNR plot. Considering coherent detection scheme, it is clear from the figure that as the number of interfering signals is increased, the system throughput drops. The enhanced performance in case of larger values of w_b/r illustrates the impact of pointing errors in the plot. This analysis is presented with model parameters fixed at $(\alpha, \mu_2) = (1, 3/2)$, while the average interference SNR is kept fixed at $\gamma_I = -7.5$ dB.

V. Conclusion

We presented a comprehensive performance analysis of dual hop mixed RF/FSO AF relaying system in the presence of co-channel interference. The RF link of the dual hop relay system is assumed to undergo η-μ fading and the atmospheric scintillations on the FSO link is modeled as α-μ distribution. For Gaussian laser beam propagating through FSO channel, closed form for the statistics have been derived for the case of zero and non-zero boresight errors. These RF and FSO channel statistics are utilized to present new analytical formulas for various performance metrics including the OP, average BER and ergodic capacity of the relay system in the presence of interference. Moreover, the asymptotic analysis of outage performance has been further extended to derive new expressions of coding gain and diversity order of the relay scheme. These results show that the overall performance of the considered system strongly depends upon FSO link model parameters α, μ_2, type of optical detection scheme, and the pointing error parameter ξ. We have validated the analytical results achieved in the work through computer-aided simulations. The insights developed in the research work provide good measure of the effect that interference can bring in FSO systems.

VI. Acknowledgment

The authors would like to thank the editor and anonymous reviewers for their valuable comments and suggestions to improve the quality of the manuscript.

Appendix A
Derivation of (20)

In order to formulate a closed form solution to (19), the Bessel's function $I_0(x)$ can be represented in summation form, using [39], as given below

$$I_0\left(\frac{\tau}{\sigma_s}\sqrt{-2\xi^2\ln\left(\frac{I}{I_a A_o}\right)}\right) = \sum_{m_1=0}^{n} \hat{b}_{m_1,n,0}\left(\frac{\tau\xi}{\sqrt{2}\sigma_s}\right)^{2m_1} \times \left\{\ln\left(\frac{I}{I_a A_o}\right)\right\}^{m_1} \tag{52}$$

where $\hat{b}_{m_1,n,0}$ has been defined in (21). After some mathematical manipulations, the integral to be addressed can be expressed as

$$f(I) = \frac{\alpha\mu}{\Gamma(\mu)\hat{\omega}}\frac{\xi^2}{{A_o}^{\xi^2}}\exp\left(-\frac{\tau^2}{2\sigma_s^2}\right)\frac{I^{\alpha\mu-1}}{A_o^{\alpha\mu-\xi^2}}\sum_{m_1=0}^{n}\hat{b}_{m_1,n,0}\left(\frac{2\tau\xi}{2\sigma_s}\right)^{2m_1} \times \int_0^\infty y^{m_1}\exp\left[-(\xi^2-\alpha\mu)y\right]\exp\left[-\Phi_0\exp\left(\alpha y\right)\right]dy \tag{53}$$

where $\Phi_0 = \frac{\mu_2}{\hat{\omega}^\alpha}\left(\frac{I}{A_o}\right)^\alpha$. Further to this, resorting to the Laplace transform theory, and the fact that if $\mathcal{L}\{.\}$ represents the Laplace transform, $\mathcal{L}\{y^{m_1}\exp\left[-\Phi_0\exp\left(-\alpha y\right)\right]\} = \frac{\partial^{m_1}}{\partial s^{m_1}}\left\{\Phi_0^s\Gamma\left(-s,\Phi_0\right)\right\}$, the closed-form expression for the PDF can be obtained as stated in (20).

Appendix B
Proof of Theorem 1

Considering γ_2 and γ_I to be independent random variables, using the definition $P_r[\gamma_1 < x] = F_{\gamma_1}(x)$, we can further express (31) as

$$P_{out} = \int_0^\infty\int_0^\infty\sum_{l=0}^{\mu_1-1}\mathcal{A}_1\Big[\mathcal{A}_2\big[1-e^{-a_1[\gamma_{th}(\gamma_I+1+\frac{C_1}{\gamma_2})]} \times\sum_{m=0}^{\mu_1-l-1}\frac{(a_1)^m}{m!}\big][\gamma_{th}(\gamma_I+1+\frac{C_1}{\gamma_2})]^m + \mathcal{A}_3\big[1-e^{-a_2\gamma_1} \times\sum_{m=0}^{\mu_1-l-1}\frac{(a_2)^m}{m!}\big][\gamma_{th}(\gamma_I+1+\frac{C_1}{\gamma_2})]^m f_{\gamma_I}(\gamma_I)f_{\gamma_2}(\gamma_2)d\gamma_I d\gamma_2\Big] \tag{54}$$

At first, we can be express $(\gamma_I + 1 + \frac{C_1}{\gamma_2})$ using the binomial expansion as per [21, Eq. (1.111)] as $\sum_{i=0}^{m}\binom{m}{i}(\gamma_I+1)^i(C_1/\gamma_2)^{m-i}$. Substituting the PDFs of γ_2 and γ_I, from (16) and (6) in (54) the requisite integrals, $\mathcal{I}_1$ and $\mathcal{I}_2$, can be formulated as

$$\mathcal{I}_1 = \int_0^\infty\frac{\gamma_I^{j+N-1}}{\bar{\gamma}_I{}^N(N-1)!}\exp\left[-\left(\frac{1}{\bar{\gamma}_I}+a_k\gamma_{th}\right)\gamma_I\right]d\gamma_I \tag{55}$$

$$\mathcal{I}_2 = \int_0^\infty\gamma_2^{\,i-m+\frac{d}{2\rho}}\exp\left(-a_kC_1\frac{\gamma_{th}}{\gamma_2}\right)d\gamma_2 \tag{56}$$

Moreover, (55) can be solved using [21, Eq. (3.381.4)], whereas for evaluating (56), the exponential functions in (56) can be expressed as $\exp\left(-\frac{a_k C_1 \gamma_{th}}{\gamma_2}\right) = \mathrm{G}_{1,0}^{0,1}\left[\frac{\gamma_2}{a_k C_1 \gamma_{th}}\middle| \begin{matrix} 1 \\ - \end{matrix}\right]$ using [28, Eq. (07.34.03.0046.01)] and $\exp\left[-\mathcal{B}_1\gamma_2^{\frac{\alpha}{\rho}}\right] = \mathrm{G}_{0,1}^{1,0}\left[\mathcal{B}_1\gamma_2^{\frac{\alpha}{\rho}}\middle| \begin{matrix} - \\ 0 \end{matrix}\right]$ as per [28, Eq. (07.34.03.0228.01)]. Finally, making use of standard identities provided in [28, Eq. (07.34.21.0013.01)] along with some mathematical manipulations, the closed form of OP can be obtained as provided in (32).

Appendix C
Proof of Theorem 2

Noting the fact that, for high SNR on the RF link, as $\bar{\gamma}_1 \to \infty$ the value of a_k diminishes, i.e., $a_k \to 0$. Therefore, the contribution of the summation in m in equation (5) is maximum at $m = 0$. Moreover, for small arguments, $\exp(-a_k\gamma_1) \simeq 1 - a_k\gamma_1$. According to definition of P_{out} in (54) along with above discussed approximations, we have

$$\begin{aligned} P_{out} &\simeq \int_0^\infty \int_0^\infty \sum_{l=0}^{\mu_1-1} \mathcal{A}_1[a_1\mathcal{A}_2 + a_2\mathcal{A}_3]\Big\{\gamma_{th}(\gamma_I+1) f_{\gamma_I}(\gamma_I) d\gamma_I\Big\} \\ &\quad + \gamma_{th}\frac{C_1}{\gamma_2} f_{\gamma_2}(\gamma_2) d\gamma_2 \\ &\simeq \sum_{l=0}^{\mu_1-1} \mathcal{A}_1[a_1\mathcal{A}_2 + a_2\mathcal{A}_3]\Big[\frac{\gamma_{th}}{\bar{\gamma}_I{}^N(N-1)!}\mathcal{I}_3 + \gamma_{th}C_1\mathcal{A}_4\mathcal{I}_4\Big] \end{aligned} \tag{57}$$

where the integrals $\mathcal{I}_3 = \int_0^\infty (\gamma_I+1)\gamma_I{}^{N-1}\exp\left[-\frac{\gamma_I}{\bar{\gamma}_I}\right]d\gamma_I$ and $\mathcal{I}_4$ can be formulated as $\mathcal{I}_2 = \int_0^\infty \gamma^{\frac{d}{2\rho}-2}\exp\left[-\mathcal{B}_1\gamma^{\frac{\alpha}{\rho}}\right]d\gamma$. With the aid of [21, Eq. (3.383.5)], we formulate a solution $\mathcal{I}_3$. On the other hand, [21, Eq. (3.478.1)] can be used to solve $\mathcal{I}_4$. The approximate expression of the OP is given as

$$\begin{aligned} P_{out} \simeq \sum_{l=0}^{\mu_1-1} \mathcal{A}_1 \Bigg[&(a_1\mathcal{A}_2 + a_2\mathcal{A}_3)\Big\{\frac{\gamma_{th}}{\bar{\gamma}_I{}^N\bar{\gamma}_1}\mathrm{U}(N, N+2, \frac{1}{\bar{\gamma}_I}) \\ &\times \frac{C_1\rho\mathcal{A}_4}{\alpha}\mathrm{B}^{-\frac{d-2\rho}{\alpha\rho}}\Gamma\Big(\frac{\rho}{\alpha}(\frac{d}{2\rho}-1)\Big)\Big\}\Bigg] \end{aligned} \tag{58}$$

After performing some mathematical manipulations and applying $\bar{\gamma}_1 \to \infty$, (58) is re-written as

$$P_{out} \simeq \sum_{l=0}^{\mu_1-1}\left[\Lambda_1\Lambda_2\kappa^{-\alpha(p_0-1)}\right]\bar{\gamma}_1{}^{-\alpha(p_0-1)-1} \tag{59}$$

From (59), along with the definitions of G_c and G_d, we can obtain the expressions given in (36) and (37), to prove Theorem 2.

Appendix D
Proof of Theorem 3

The exact expression of the end-to-end CDF of the dual hop relaying strategy can be obtained by putting $\gamma_{th} = \gamma$ in (32). Moreover, substituting the end-to-end CDF of the mixed RF/FSO system into (40), the intermediate expression for the average BER of the system can be further expressed as

$$\begin{aligned} \bar{P}_b = \sum_{l=0}^{\mu_1-1}\frac{q^p\mathcal{A}_1}{2\Gamma(p)}\Bigg[&\mathcal{A}_2\Big\{\mathcal{I}_3 - \sum_{m}^{\mu_1-l-1}\sum_{i=0}^{m}\sum_{j=0}^{i}\mathcal{I}_{4,1}\Big\} + \mathcal{A}_3\Big\{\mathcal{I}_3 \\ &- \sum_{m}^{\mu_1-l-1}\sum_{i=0}^{m}\sum_{j=0}^{i}\mathcal{I}_{4,2}\Big\}\Bigg] \end{aligned} \tag{60}$$

where $\mathcal{I}_3 = \int_0^\infty \gamma^{p-1}\exp(-q\gamma)d\gamma = q^{-p}\Gamma(p)$ while second integral is given as

$$\begin{aligned} \mathcal{I}_{4,k} = &\int_0^\infty \gamma^{\frac{d}{2\rho}+p-1}\exp[-\gamma\Big(q+a_k\Big)]\Big[\frac{1}{\bar{\gamma}_I} + \gamma a_k\Big]^{-N-j} \\ &\times \mathrm{G}_{0,g+h}^{g+h,0}\left[B_{2,k}\gamma^h\middle| \begin{matrix} - \\ k_1 \end{matrix}\right]d\gamma \end{aligned} \tag{61}$$

On representing $\left[\frac{1}{\bar{\gamma}_I} + \frac{\gamma_{th}}{\bar{\gamma}_1}\right]^{-N} = \frac{\bar{\gamma}_I{}^N}{N!}\mathrm{G}_{1,1}^{1,1}\left[\frac{\gamma\bar{\gamma}_I}{\bar{\gamma}_1}\middle| \begin{matrix} 1-N \\ 0 \end{matrix}\right]$ and expressing $\exp\left[-\gamma\Big(q+\frac{1}{\bar{\gamma}_1}\Big)\right] = \mathrm{G}_{0,1}^{1,0}\left[\gamma\Big(q+\frac{1}{\bar{\gamma}_1}\Big)\middle| \begin{matrix} - \\ 0 \end{matrix}\right]$ by the using [28, Eq. (07.34.03.0271.01)] and [28, Eq. (07.34.03.0228.01)], respectively, the integral in (43) can be further expressed as

$$\begin{aligned} \mathcal{I}_4 = &\int_0^\infty \gamma^{\frac{d}{2\rho}+p-1}\mathrm{G}_{0,1}^{1,0}\left[\gamma\Big(q+\frac{1}{\bar{\gamma}_1}\Big)\middle| \begin{matrix} - \\ 0 \end{matrix}\right]\mathrm{G}_{1,1}^{1,1}\left[\frac{\gamma\bar{\gamma}_I}{\bar{\gamma}_1}\middle| \begin{matrix} 1-N \\ 0 \end{matrix}\right] \\ &\times \mathrm{G}_{0,g+h}^{g+h,0}\left[B_1\gamma^h\middle| \begin{matrix} - \\ k_1 \end{matrix}\right]d\gamma \end{aligned} \tag{62}$$

Finally, by representing each Meijer-G function in terms of Fox's H function on account of [28, Eq (07.34.26.0008.01)], the integral $\mathcal{I}_{4,k}$ can be solved by applying the identity [32, Eq. (2.3)] to yield (27).

Appendix E
Proof of Theorem 4

Plugging (46) into (45) reveals that the computation of ergodic capacity $\bar{C}$ requires the solution of integrals of the form given below:

$$\begin{aligned} \mathcal{I}_{5,k} = &\int_0^\infty \gamma^{\frac{d}{2\rho}}\exp(-a_k\gamma)\log_2(1+\delta\gamma)\Big[\frac{1}{\bar{\gamma}_I} + \gamma a_k\Big]^{-N-s_1} \\ &\times \mathrm{G}_{0,g+h}^{g+h,0}\left[B_{2,k}\gamma^h\middle| \begin{matrix} - \\ k_1 \end{matrix}\right]d\gamma \end{aligned} \tag{63}$$

By expressing $\log_2(1+\delta\gamma) = (1/\ln(2))\mathrm{G}_{2,2}^{1,2}\left[\delta\gamma\middle| \begin{matrix} 1,1 \\ 1,0 \end{matrix}\right]$ using [28, Eq. (07.34.03.0456.01)] and by substituting $\left[\frac{1}{\bar{\gamma}_I} + \gamma a_k\right]^{-N-s_1} = [\bar{\gamma}_I{}^{s_1+N}/\Gamma(s_1+N)]\mathrm{G}_{1,1}^{1,1}\left[\gamma a_k\bar{\gamma}_I\middle| \begin{matrix} 1-N-s_1 \\ 0 \end{matrix}\right]$ by the help of [28, Eq. (07.34.03.0271.01)], the integral $\mathcal{I}_{5,k}$ in (63), can be formulated as

$$\begin{aligned} \mathcal{I}_{5,k} = &[\bar{\gamma}_I{}^{s_1+N}/\Gamma(s_1+N)]\int_0^\infty \gamma^{\frac{d}{2\rho}}\exp(-\gamma a_k)\,\mathrm{G}_{2,2}^{1,2}\left[\delta\gamma\middle| \begin{matrix} 1,1 \\ 1,0 \end{matrix}\right] \\ &\times \mathrm{G}_{1,1}^{1,1}\left[\gamma a_k\bar{\gamma}_I\middle| \begin{matrix} 1-N-s_1 \\ 0 \end{matrix}\right]\mathrm{G}_{0,g+h}^{g+h,0}\left[B_{2,k}\gamma^h\middle| \begin{matrix} - \\ k_1 \end{matrix}\right]d\gamma \end{aligned} \tag{64}$$

After converting the Meijer-G functions into Fox-H function with the aid of [28, Eq (07.34.26.0008.01)], a closed-form solution of (64) can be obtained by representing each Fox-H

function in complex integral form with the aid of [32, Eq. (2.1)] as given below

$$\mathrm{G}_{2,2}^{1,2}\left[\delta\gamma\middle|\begin{smallmatrix}1,1\\1,0\end{smallmatrix}\right]=\frac{1}{2\pi i}\int_{\mathcal{L}_1}\Gamma(z_1)\Gamma(1-z_1)(\delta\gamma)^{-z_1}dz_1 \tag{65}$$

$$\mathrm{G}_{1,1}^{1,1}\left[\gamma a_k\bar{\gamma}_I\middle|\begin{smallmatrix}1-N-z_1\\0\end{smallmatrix}\right]=\frac{1}{2\pi i}\int_{\mathcal{L}_2}\Gamma(z_2)\Gamma(N-z_2)\left(\gamma a_k\bar{\gamma}_I\right)^{-z_2}dz_2 \tag{66}$$

$$\mathrm{G}_{0,g+h}^{g+h,0}\left[B_{2,k}\gamma^h\middle|\begin{smallmatrix}\\k_1\end{smallmatrix}\right]=\frac{1}{2\pi i}\int_{\mathcal{L}_3}\prod_{j=1}^{g+h}\Gamma(k_{1,j}-z_3)\left(B_1\gamma^h\right)^{-z_3}dz_3 \tag{67}$$

Putting the above expressions (65, 66, 67) in (64), the overall complex integral can be expressed as provided in (68). On utilizing [21, Eq. (3.381.4)] to solve the inner integral and making use of [38, Eq. (28-30)], a closed-form solution to (68) in terms of trivariate Fox-H function can be obtained to prove Theorem 4.

Appendix F
Derivation of 50 and 51

Noting the fact that the solution to (63) results into the expression of $\mathcal{J}_{1,k}$, we firstly resort to approximate (63) for high SNR regime. Making use of [28, 07.34.06.0006.01] to approximate Meijer-G in (63), we have

$$\mathcal{I}_{5,k}\simeq\int_0^\infty\gamma^{\frac{d}{2\rho}}\exp\left(-a_k\gamma\right)\log_2(1+\delta\gamma)\left[\frac{1}{\bar{\gamma}_I}+\gamma a_k\right]^{-N-s_1}\times\sum_{j_1=1}^{g+h}\prod_{j_2=1,j_1\neq j_2}^{g+h}\Gamma(k_{2,j_2}-k_{2,j_1})[\mathcal{B}_{2,k}\gamma]^{k_{2,j_1}}d\gamma \tag{69}$$

Moreover, after representing Fox's H-function representation of $(1+\delta\gamma)$, $\left[\frac{1}{\bar{\gamma}_I}+\gamma a_k\right]^{-N-s_1}$ and resorting to the Mellin-Barnes representation of the Fox's H-function as per [34, Eq. (1.2-1.3)], we formulate the above integral as

$$\mathcal{I}_{5,k}\simeq\sum_{j_1=1}^{g+h}\prod_{j_2=1,j_1\neq j_2}^{g+h}\frac{\Gamma(k_{2,j_2}-k_{2,j_1})(\mathcal{B}_{2,k})^{k_{2,j_1}}\bar{\gamma}_I^{s_1N}a_k{}^{-p_2}}{(2\pi i)^2\Gamma(s_1+N)}\times\int_{\mathcal{L}_1}\int_{\mathcal{L}_2}\underbrace{\int_0^\infty\gamma^{p_2-z_2-z_1}e^{-a_k\gamma}d\gamma}\,\Gamma(z_1)\Gamma(s_1+N-z_1)\times\left(a_k\bar{\gamma}_I\right)^{-z_1}\frac{\Gamma(1+z_2)\Gamma^2(-z_2)}{\Gamma(1-z_2)}\delta^{-z_2}dz_1dz_2 \tag{70}$$

Inner integral can be solved by utilizing [21, Eq. (3.381.4)], after following the same procedure as utilized in deriving (44) by obtaining the residue of (70) at the most negative pole β yields (50). The asymptotic expression for $\mathcal{J}_{2.k}$ follows in the same line of (50).

References

[1] A. A. Farid and S. Hranilovic, "Outage capacity optimization for free-space optical links with pointing errors," *Journal of Lightwave Technology*, vol. 25, no. 7, pp. 1702–1710, July 2007.

[2] S. R. Z. Ghassemlooy, W. Popoola, "Optical wireless communications: system and channel modeling with MATLAB," *CRC Press*, 2012.

[3] E. Lee, J. Park, D. Han, and G. Yoon, "Performance analysis of the asymmetric dual-hop relay transmission with mixed RF/FSO links," *IEEE Photonics Technology Letters*, vol. 23, no. 21, pp. 1642–1644, Nov. 2011.

[4] I. S. Ansari, F. Yilmaz, and M. S. Alouini, "Impact of pointing errors on the performance of mixed RF/FSO dual-hop transmission systems," *IEEE Wireless Communications Letters*, vol. 2, no. 3, pp. 351–354, June 2013.

[5] E. Zedini, I. S. Ansari, and M. S. Alouini, "Performance analysis of mixed Nakagami-m and Gamma Gamma dual-hop FSO transmission systems," *IEEE Photonics Journal*, vol. 7, no. 1, pp. 1–20, Feb. 2015.

[6] G. Djordjevic, M. Petkovic, A. Cvetkovic, and G. Karagiannidis, "Mixed RF/FSO relaying with outdated channel state information," *IEEE Journal on Selected Areas in Communications*, vol. PP, no. 99, pp. 2860–2867, Sept. 2015.

[7] A. H. A. El-Malek, A. M. Salhab, S. A. Zummo, and M. S. Alouini, "Security-reliability trade-off analysis for multiuser SIMO mixed RF/FSO relay networks with opportunistic user scheduling," *IEEE Transactions on Wireless Communications*, vol. 15, no. 9, pp. 5904–5918, Sept. 2016.

[8] P. Wang, R. Wang, L. Guo, T. Cao, and Y. Yang, "On the performances of relay-aided FSO system over $\mathcal{M}$ distribution with pointing errors in presence of various weather conditions," *Optics Communications*, vol. 367, pp. 59–67, May 2016.

[9] E. Soleimani-Nasab and M. Uysal, "Generalized performance analysis of mixed RF/FSO cooperative systems," *IEEE Transactions on Wireless Communications*, vol. 15, no. 1, pp. 714–727, Jan. 2016.

[10] M. I. Petkovic, A. M. Cvetkovic, G. T. Djordjevic, and G. K. Karagiannidis, "Outage performance of the mixed RF/FSO relaying channel in the presence of interference," *Wireless Pers Commun, Springer*, vol. 96, no. 2, pp. 2999–3014, Sept. 2017.

[11] N. Cherif, I. Trigui, and S. Affes, "On the performance analysis of mixed multi-aperture FSO/multiuser RF relay systems with interference," *Proceedings Signal Processing Advances in Wireless Communications*, pp. 1–5, Jul. 2017.

[12] E. Balti and M. Guizani, "Mixed RF/FSO cooperative relaying systems with co-channel interference," *IEEE Transactions on Communications*, vol. 66, no. 9, pp. 4014–4027, 2018.

[13] A. Upadhya, V. K. Dwivedi, and G. Singh, "Multiuser diversity for mixed RF/FSO cooperative relaying in the presence of interference," *Optics Communications*, vol. 442, pp. 77 – 83, 2019.

[14] M. D. Yacoub, "The $\kappa-\mu$ distribution and the $\eta-\mu$ distribution," *IEEE Antennas and Propagation Magazine*, vol. 49, no. 1, pp. 68–81, Feb 2007.

[15] ——, "The $\alpha-\mu$ distribution: A physical fading model for the stacy distribution," *IEEE Transactions on Vehicular Technology*, vol. 56, no. 1, pp. 27–34, Jan. 2007.

[16] U. S. Dias and M. D. Yacoub, "On the $\alpha-\mu$ autocorrelation and power spectrum functions: Field trials and validation," *GLOBECOM 2009 - 2009 IEEE Global Telecommunications Conference*, pp. 1–6, 2009.

[17] K. P. Peppas, A. N. Stassinakis, H. E. Nistazakis, and G. S. Tombras, "Capacity analysis of dual amplify-and-forward relayed free-space optical communication systems over turbulence channels with pointing errors," *IEEE/OSA Journal of Optical Communications and Networking*, vol. 5, no. 9, pp. 1032–1042, Sept. 2013.

[18] R. Boluda-Ruiz, A. Garcia-Zambrana, B. Castillo-Vazquez, and C. Castillo-Vazquez, "Ergodic capacity analysis of decode-and-forward relay-assisted FSO systems over $\alpha-\mu$ fading channels considering pointing errors," *IEEE Photonics Journal*, vol. 8, no. 1, pp. 1–11, Feb. 2016.

[19] A. Upadhya, V. K. Dwivedi, and G. Singh, "Relay-aided free-space optical communications using $\alpha-\mu$ distribution over atmospheric turbulence channels with misalignment errors," *Optics Communication, Elsevier*, vol. 416, pp. 117–124, June 2018.

[20] F. Yang, J. Cheng, and T. A. Tsiftsis, "Free-space optical communication with nonzero boresight pointing errors," *IEEE Trans. Commun.*, vol. 62, no. 2, pp. 713–725, Feb. 2014.

[21] I. S. Gradshteyn and I. M. Ryzhik, "Table of integrals, series and products," *New York, NY, USA: Academic*, 2000.

[22] T. A. Tsiftsis, F. Foukalas, G. K. Karagiannidis, and T. Khattab, "On the higher-order statistics of the channel capacity in dispersed spectrum cognitive radio systems over generalized fading channels," *IEEE Trans. Veh. Technol*, vol. 65, no. 5, pp. 3818–3823, May 2016.

[23] M. O. Hasna, M. S. Alouini, A. Bastami, and E. S. Ebbini, "Performance analysis of cellular mobile systems with successive co-channel interference cancellation," *IEEE Transactions on Wireless Communications*, vol. 2, no. 1, pp. 29–40, Jan. 2004.

[24] H. G. Sandalidis, T. A. Tsiftsis, G. K. Karagiannidis, and M. Uysal, "BER performance of FSO links over strong atmospheric turbulence channels with pointing errors," *IEEE Communications Letters*, vol. 12, no. 1, pp. 44–46, Jan. 2008.

$$\mathcal{I}_{5,k} = \int_{\mathcal{L}_1}\int_{\mathcal{L}_2}\int_{\mathcal{L}_3}\left[\int_0^{\infty}\gamma^{\frac{d}{2\rho}-z_1-z_2-hz_3}e^{-\gamma a_k}d\gamma\right]\frac{\Gamma(z_1)\Gamma(1-z_1)\Gamma(z_2)\Gamma(N-z_2)}{(2\pi i)^3}\prod_{j=1}^{g+h}\Gamma(k_{1,j}-z_3)(\delta)^{-z_1}\left(a_k\bar{\gamma}_t\right)^{z_2}\left(B_1\right)^{-z_3}dz_1dz_2dz_3 \tag{68}$$

[25] M. A. Al-Habash, L. C. Andrews, and R. L. Phillips, "Mathematical model for the irradiance PDF of a laser beam propagating through turbulent media," *Opt. Eng*, vol. 40, no. 8, pp. 1554–1562, Aug. 2001.

[26] K. Kiasaleh, "Performance of coherent DPSK free-space optical communication systems in K-distributed turbulence," *IEEE Transactions on Communications*, vol. 54, no. 4, pp. 604–607, April 2006.

[27] L. Yang, X. Gao, and M. Alouini, "Performance analysis of free-space optical communication systems with multiuser diversity over atmospheric turbulence channels," *IEEE Photonics Journal*, vol. 6, no. 2, pp. 1–17, April 2014.

[28] I. Wolfram, "Wolfram, research, mathematica edition: Version 10.0. champaign," *Wolfram Research, Inc.*, 2010.

[29] M. A. Kashani, M. Safari, and M. Uysal, "Optimal relay placement and diversity analysis of relay-assisted free-space optical communication systems," *IEEE/OSA Journal of Optical Communications and Networking*, vol. 5, no. 1, pp. 32–47, Jan. 2013.

[30] Z. Wang and G. B. Giannakis, "A simple and general parameterization quantifying performance in fading channels," *IEEE Transactions on Communications*, vol. 51, no. 8, pp. 1389–1398, Aug. 2003.

[31] I. S. Ansari, S. Al-Ahmadi, F. Yilmaz, M.-S. Alouini, and H. Yanikomeroglu, "A new formula for the BER of binary modulations with dual-branch selection over generalized-K composite fading channels," *IEEE Transaction on Communications*, vol. 59, no. 10, pp. 2654–2658, Oct. 2011.

[32] P. Mittal and K. Gupta, "An integral involving generalized function of two variables," *Proceedings of the Indian Academy of Sciences - Section A*, vol. 75, no. 3, pp. 117–123, Nov. 1972.

[33] K. P. Peppas, "A new formula for the average bit error probability of dual-hop amplify-and-forward relaying systems over generalized shadowed fading channels," *IEEE Wireless Communications Letters*, vol. 1, no. 2, pp. 85–88, April 2012.

[34] A. Kilbas, "H-transforms: Theory and applications. analytical methods and special functions," *Taylor and Francis*, 2004.

[35] A. Annamalai, R. C. Palat, and J. Matyjas, "Estimating ergodic capacity of cooperative analog relaying under different adaptive source transmission techniques," *2010 IEEE Sarnoff Symposium*, pp. 1–5, April 2010.

[36] A. Lapidoth, S. M. Moser, and M. A. Wigger, "On the capacity of free space optical intensity channels," *IEEE Transactions on Information Theory*, vol. 55, no. 10, pp. 4449–4461, Oct. 2009.

[37] H. M. Srivastava and R. Panda, "Some bilateral generating functions for a class of generalized hypergeometric polynomials," *J. Reine Angew. Math.*, pp. 283–284, June 1976.

[38] H. R. Alhennawi, M. M. H. E. Ayadi, M. H. Ismail, and H. A. M. Mourad, "Closed-form exact and asymptotic expressions for the symbol error rate and capacity of the H-function fading channel," *IEEE Transactions on Vehicular Technology*, vol. 65, no. 4, pp. 1957–1974, April 2016.

[39] L.-L. Li, F.L, and F. Gross, "A new polynomial approximation for jn bessel functions," *Applied Mathematics and Computation*, vol. 183, no. 2, pp. 1220–1225, April 2006.

Abhijeet Upadhya received his B.Tech. and M. Tech. degrees in Electronics and Communications engineering from AKTU, India. He is currently a research scholar in Jaypee Institute of Information Technology, Noida, India and is working as Assistant Professor in Electronics and Communication Engineering department at Ajay Kumar Garg Engineering College, Ghaziabad, India. His research interests include wireless communication systems, cooperative relaying and free space optical communication systems. Other areas of research include statistical characterization and modeling of wireless fading channels and performance evaluation of digital wireless communication systems subject to interference.

Vivek K. Dwivedi received a Bachelor of Engineering from the RGPV, Bhopal, India, Master of Engineering from Birla Institute of Technology, Mesra, Ranchi, India and his Ph.D. in Electronics and Communication Engineering from Jaypee University of Information Technology, Solan, India, in 2003, 2006 and 2012, respectively. He was a senior visiting researcher in Wireless Communications at the University of Pretoria, South Africa from 2014 to 2015. He is currently working as an Associate Professor in the Department of Electronics and Communication Engineering at Jaypee Institute of Information Technology, Noida, India. He has authored several research papers in refereed international journals and conferences. His primary research interest includes machine learning, artificial intelligence, 5G, and optical wireless communication. He is a member of IEEE and is serving as an Associate Editor of the IEEE Access Journal.

George K. Karagiannidis was born in Pithagorion, Samos Island, Greece. He received the University Diploma (5 years) and PhD degree, both in electrical and computer engineering from the University of Patras, in 1987 and 1999, respectively. From 2000 to 2004, he was a Senior Researcher at the Institute for Space Applications and Remote Sensing, National Observatory of Athens, Greece. In June 2004, he joined the faculty of Aristotle University of Thessaloniki, Greece where he is currently Professor in the Electrical & Computer Engineering Dept. and Director of Digital Telecommunications Systems and Networks Laboratory. He is also Honorary Professor at South West Jiaotong University, Chengdu, China.

His research interests are in the broad area of Digital Communications Systems and Signal processing, with emphasis on Wireless Communications, Optical Wireless Communications, Wireless Power Transfer and Applications, Molecular and Nanoscale Communications, Stochastic Processes in Biology and Wireless Security. He is the author or co-author of more than 450 technical papers published in scientific journals and presented at international conferences. He is also author of the Greek edition of a book on "Telecommunications Systems" and co-author of the book "Advanced Optical Wireless Communications Systems", Cambridge Publications, 2012.

Dr. Karagiannidis has been involved as General Chair, Technical Program Chair and member of Technical Program Committees in several IEEE and non-IEEE conferences. In the past, he was Editor in IEEE Transactions on Communications, Senior Editor of IEEE Communications Letters, Editor of the EURASIP Journal of Wireless Communications & Networks and several times Guest Editor in IEEE Selected Areas in Communications. From 2012 to 2015 he was the Editor-in Chief of IEEE Communications Letters.

Dr. Karagiannidis is IEEE Fellow and one of the highly-cited authors across all areas of Electrical Engineering, recognized as 2015, 2016 and 2017 Web-of-Science Highly-Cited Researcher.